University of Nevada

Reno

Geology and Geochemistry of the Almanor and Glidden Barite

Deposits, Northern California

A Thesis submitted in partial fulfillment of the

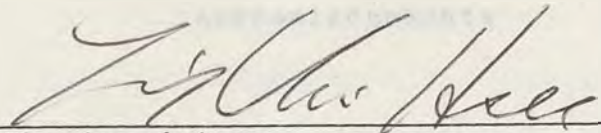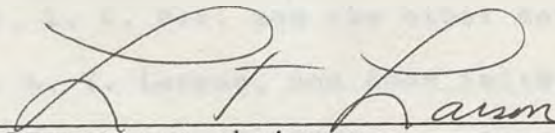requirements for the degree of Master of Science
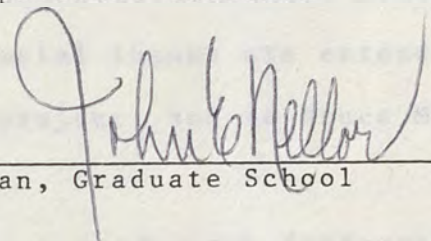
in Geology

by

John Bradley Wigglesworth

March 1984

The thesis of John Bradley Wigglesworth is aproved:

_____
Thesis advisor

_____
Department chairman

_____
Dean, Graduate School

University of Nevada

Reno

March, 1984

Acknowledgements

ABSTRACT

The Almanor and Glidden bedded barite deposits are at the northern end of a 700 km long "California barite belt", and are associated with siliceous sediments and volcanic arc derived rocks of Devonian (?) and middle Devonian age respectively. Regional geologic relations allow correlation of these deposits with similar deposits of north central Nevada.

Geochemical evidence suggests a hydrothermal source for the barium. Cyclic stratigraphic variations in the strontium content of barite from the Glidden deposit may be the result of cyclic temporal variations in the physico-chemical environment of mineralization.

TABLE OF CONTENTS

LIST OF FIGURES

LIST OF TABLES

INTRODUCTION

Barite is found, at the Almanor and Glidden deposits, as distinctly conformable lenticular bodies intercalated within fine grained siliceous sediments of Devonian (?) and middle Devonian age, respectively. According to Brobst's (1975) classification scheme they are bedded deposits.

The purpose of this thesis is to describe certain geologic and geochemical aspects of these deposits, and to offer an explanation regarding their origin. Fieldwork for this study was conducted during the summers of 1982 and 1983. Laboratory work was carried out during the fall of 1982, and spring of 1983.

The Almanor bedded barite deposit is in northern Plumas County, California, approximately 5 km south of Lake Almanor; the Glidden bedded barite deposit is in northern Shasta County, California, approximately 8 km southeast of Castle Crags State Park (Figure 1). Both areas are characterized by a thick vegetation cover which generally limits bedrock exposures to road cuts and mine workings.

According to Diller (1892) reconnaisance parties of the California Geological Survey passed through the Almanor area in 1861 and 1863. The first systematic geologic study of the Almanor area started in 1890 and was published in 1892 (Diller, 1892). Turner, (1894, 1896, 1897) also provides numerous geologic descriptions of this area.
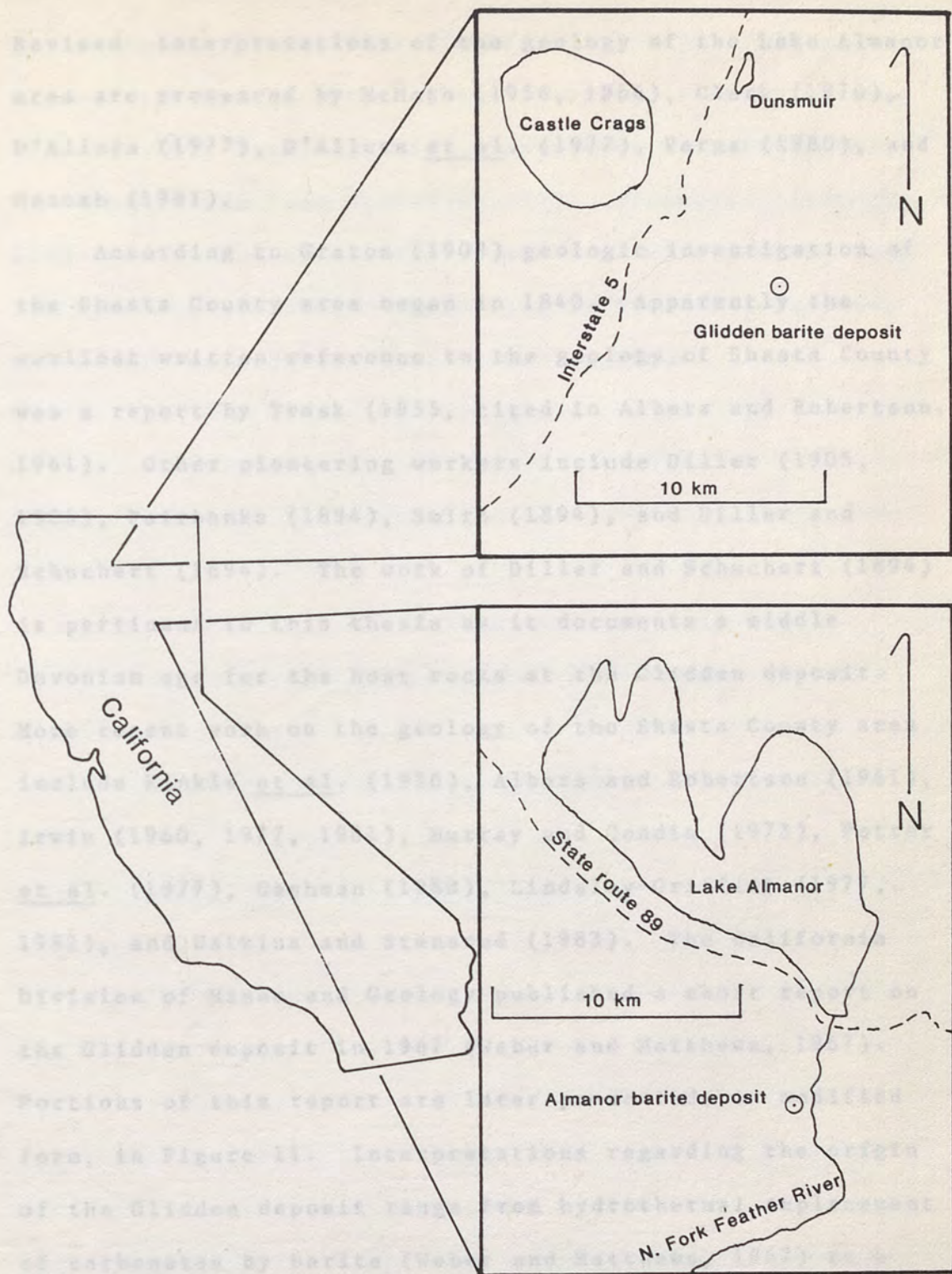
Figure 1 Location of the Almanor and Glidden bedded barite deposits.

Revised interpretations of the geology of the Lake Almanor
area are presented by McMath (1958, 1966), Clark (1976),
D'Allura (1977), D'Allura et al. (1977), Varga (1980), and
Hannah (1981).

According to Graton (1909) geologic investigation of
the Shasta County area began in 1840. Apparently the
earliest written reference to the geology of Shasta County
was a report by Trask (1855, cited in Albers and Robertson,
1961). Other pioneering workers include Diller (1905,
1906), Fairbanks (1894), Smith (1894), and Diller and
Schuchert (1894). The work of Diller and Schuchert (1894)
is pertinent to this thesis as it documents a middle
Devonian age for the host rocks at the Glidden deposit.
More recent work on the geology of the Shasta County area
include Kinkle et al. (1956), Albers and Robertson (1961),
Irwin (1960, 1977, 1981), Murray and Condie (1973), Potter
et al. (1977), Cashman (1980), Lindsley-Griffith (1977,
1982), and Watkins and Stensrud (1983). The California
Division of Mines and Geology published a short report on
the Glidden deposit in 1967 (Weber and Matthews, 1967).
Portions of this report are later presented, in modified
form, in Figure 11. Interpretations regarding the origin
of the Glidden deposit range from hydrothermal replacement
of carbonates by barite (Weber and Matthews, 1967) to a
syngenetic exhalative theory (Averill, 1939).

Production from the Almanor deposit has totaled

approximately 25,000 tons of 94% to 95% $BaSO_4$ from two mines: the Kansas mine and the Synthetic Iron Color mine (Weber, 1963; Averill, 1937). According to Weber (1963) the deposit was last worked in 1953. Production from the Glidden deposit has totaled 30,000 tons of 93% $BaSO_4$ from one mine (Weber, 1963). According to Weber and Matthews (1967) the deposit was last worked in 1966.

REGIONAL GEOLOGIC SETTING

The Almanor and Glidden bedded barite deposits are approximately 175 km apart and lie at the northern end of a discontinuous barite belt, about 700 km long, associated with rocks of Paleozoic and Paleozoic (?) age (Figure 2). The Almanor deposit is in regionally metamorphosed Paleozoic rocks of the northern Sierras, and the Glidden deposit is in similar rocks in the Eastern Klamath Subprovince of Irwin's (1960) Klamath Mountains Province (Figure 2).

The close resemblence of these two widely separated deposits, documented for the first time in this thesis, suggests a regionally distributed source for the barium. A knowledge of the regional geologic setting may be useful in identifying such a source.

Northern Sierras

Paleozoic and Mesozoic rocks of the northern Sierras lie north and west of the main mass of the Sierra Nevada Batholith and are bounded on the west by the Melones fault zone (Figure 3). The rocks of this belt range in age from Eocambrian (?) to Triassic (Schweickert, 1981). However, regional metamorphism during the late Jurassic Nevadan Orogeny (Hannah and Verosub, 1980) and the generally unfossiliferous nature of the pre-late Devonian rocks
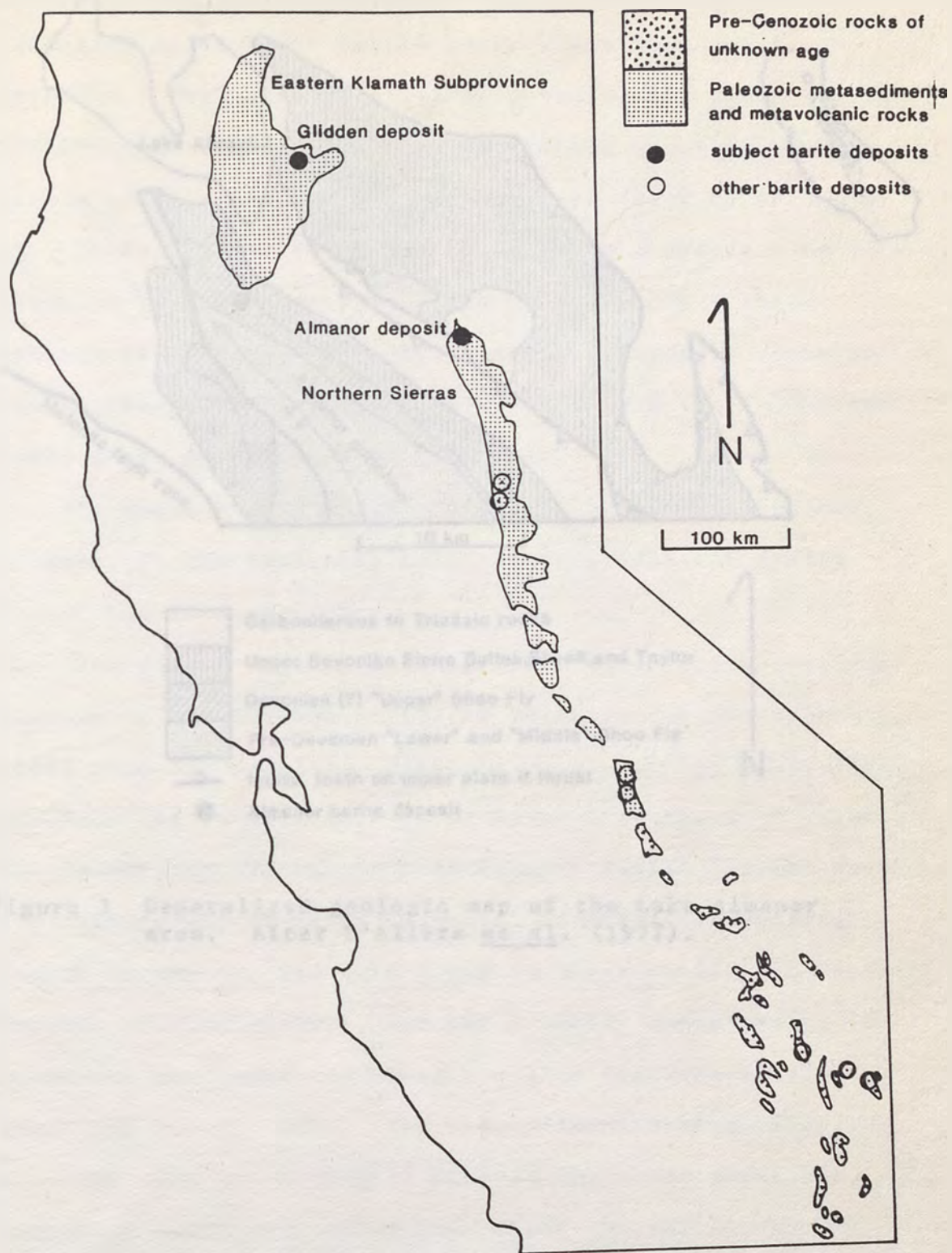
Figure 2   Generalized geologic map of the California barite belt.   After Weber (1966); Schweickert (1981).

Legend:
- Carboniferous to Triassic rocks
- Upper Devonian Sierra Buttes,Elwell,and Taylor
- Devonian (?) "Upper" Shoo Fly
- Pre-Devonian "Lower" and "Middle" Shoo Fly
- faults, teeth on upper plate if thrust
- Almanor barite deposit

Lake Almanor

Melones fault zone

Almanor anticline

10 km

N
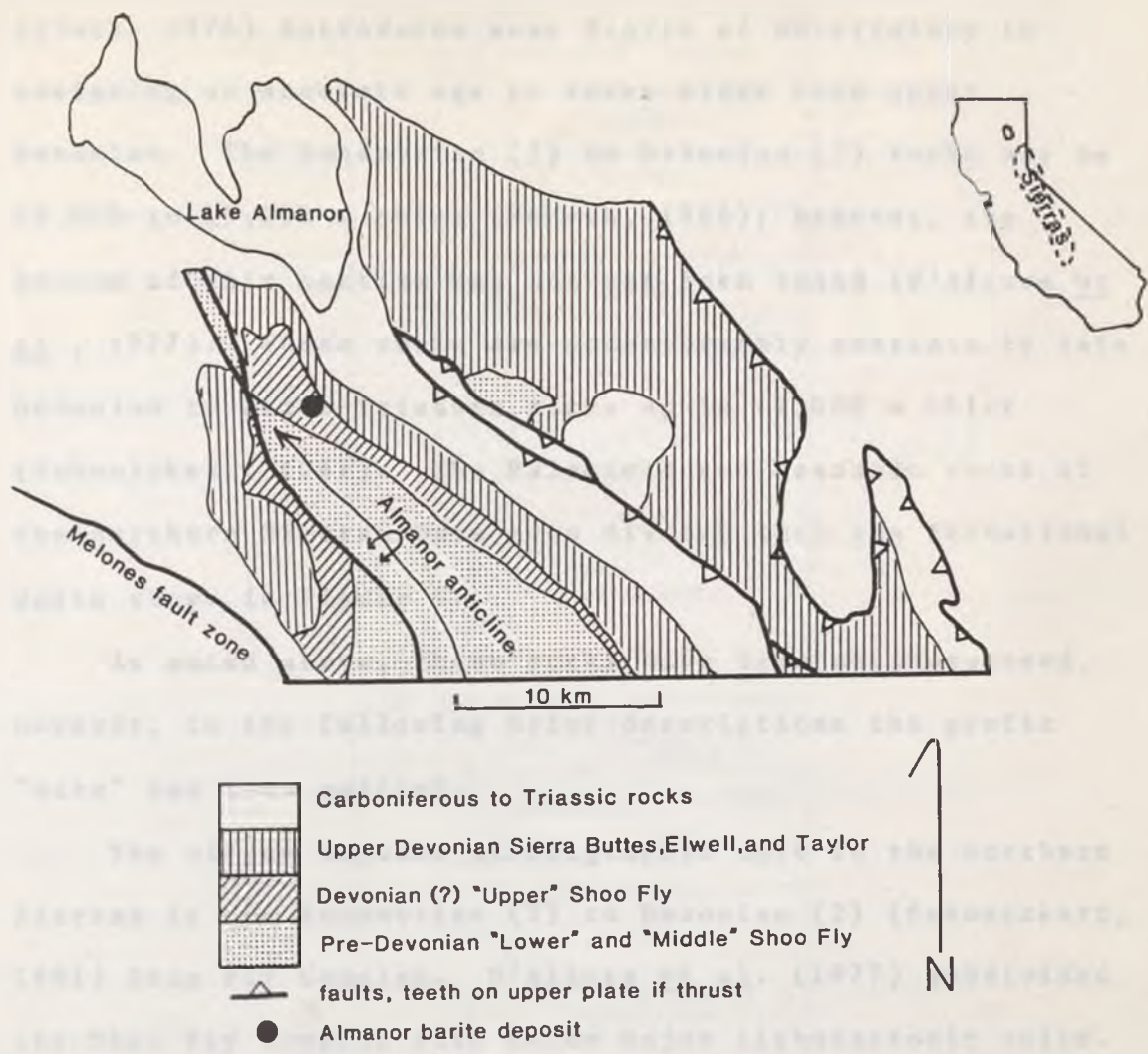
Figure 3 Generalized geologic map of the Lake Almanor
area. After D'Allura et al. (1977).

(Clark, 1976) introduces some degree of uncertainty in assigning an accurate age to rocks older than upper Devonian. The Eocambrian (?) to Devonian (?) rocks may be 12,000 to 15,000 m thick (McMath, 1966); however, the bottom of this section has not yet been found (D'Allura et al., 1977). These rocks are unconformably overlain by late Devonian to Permo-Triassic rocks up to 11,000 m thick (Schweickert, 1981). The Paleozoic and Mesozoic rocks of the northern Sierras have been divided into the formational units shown in Figure 4.

As noted above, these rocks have been metamorphosed, however, in the following brief descriptions the prefix "meta" has been omitted.

The oldest exposed stratigraphic unit in the northern Sierras is the Eocambrian (?) to Devonian (?) (Schweickert, 1981) Shoo Fly Complex. D'Allura et al. (1977) subdivided the Shoo Fly Complex into three major lithotectonic units. The Eocambrian (?) to pre Ordovician-Silurian "lower" Shoo Fly is composed of subfeldspathic and lithic sandstone, quartz sandstone, and dark green to black shale with lesser amounts of conglomerate, and was probably deposited in submarine fan complexes along a stable continental margin (Bond and Devey, 1980). The Ordovician-Silurian "middle" Shoo Fly consists of highly sheared shale and sandstone, lenses of limestone, dolostone, chert and volcanics, and small masses of serpentinized ultramafic rocks, and
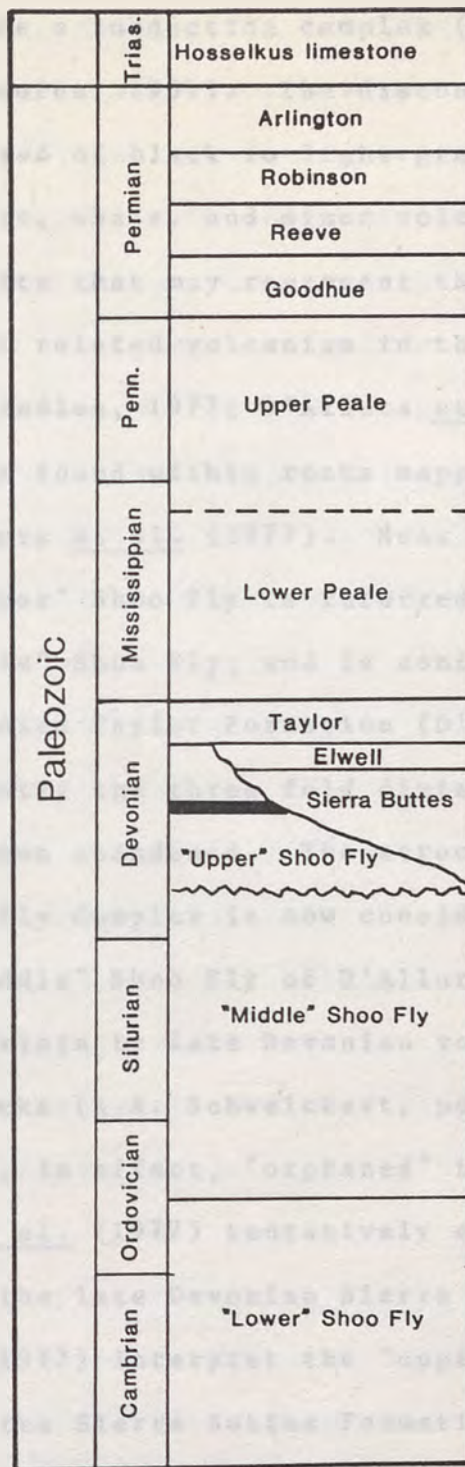
Figure 4 Stratigraphy of the northern Sierras. Heavy line shows position of Almanor bedded barite. After D'Allura et al. (1977).

probably represents a subduction complex (D'Allura et al., 1977; Varga and Moores, 1981). The discontinuous "upper" Shoo Fly is composed of black to light gray chert, siliceous argillite, shale, and minor volcanic and volcaniclastic units that may represent the first clear development of arc related volcanism in the Sierra region (McMath, 1966; Standlee, 1977; D'Allura et al., 1977). The Almanor deposit is found within rocks mapped as "upper" Shoo Fly by D'Allura et al. (1977). Near Lake Almanor the discontinuous "upper" Shoo Fly is inferred to unconformably overlie the "middle" Shoo Fly, and is conformable with the younger late Devonian Taylor Formation (D'Allura et al., 1977). More recently the three fold division of the Shoo Fly Complex has been abandoned. The structurally highest unit in the Shoo Fly Complex is now considered to be a melange unit ("middle" Shoo Fly of D'Allura et al., 1977) unconformably overlain by late Devonian volcanic and volcaniclastic rocks (R.A. Schweickert, pers. comm., 1983). This revision has, in effect, "orphaned" the "upper" Shoo Fly. D'Allura et al. (1977) tentatively suggest correlation with the late Devonian Sierra Buttes Formation, and Bond et al. (1977) interpret the "upper" Shoo Fly as "a distal facies of the Sierra Buttes Formation produced by an early phase of siliceous volcanism". However, the "upper" Shoo Fly is similar, in many respects, to the Grizzly Formation as redefined by McMath (1958, 1966). The Grizzly

Formation, exposed approximately 25 km southeast of the Almanor deposit, is a thin discontinuous unit composed of shale, siltstone, and quartz rich wacke that unconformably overlies the "middle (?)" Shoo Fly and is gradational with the overlying Sierra Buttes Formation (McMath, 1958, 1966).

Unconformably overlying the "middle (?)" Shoo Fly is a collection of Devonian to Permo-Triassic volcanic and volcaniclastic rocks, about 11,000 m thick, deposited in a volcanic island arc setting (Schweickert, 1981). This pyroclastic sequence is composed of two volcanic phases: an older Devonian phase consisting of the "upper" Shoo Fly (?), Sierra Buttes, Elwell, and Taylor Formations, and a younger Permo-Triassic phase consisting of the Goodhue, Reeve, Robinson, and Arlington Formations (D'Allura et al., 1977). Separating these dominantly volcanic units is the Carboniferous Peale Formation. The upper part of the Peale Formation is composed of chert and fine grained clastic sediments, and may represent a period of slow pelagic sedimentation (D'Allura et al., 1977).

Eastern Klamaths

Paleozoic and Mesozoic rocks of the Eastern Klamath Subprovince lie east of the Trinity thrust fault and are bounded to the south, east, and north by unconformably overlying Cretaceous and younger rocks (Figure 5). These rocks range in age from Ordovician to Jurassic and may be

Figure 5 Generalized geologic map of the Eastern Klamath
Subprovince. After Murray and Condie (1973).

up to 15,000 m thick (Irwin, 1977, 1981).

The oldest exposed stratigraphic unit in the Eastern Klamath Subprovince is the Ordovician Trinity Ophiolite (Hopson and Mattinson, 1973). The Trinity Ophiolite is composed of ultramafic to mafic plutonic and volcanic rocks and is thought to represent oceanic crust and upper mantle material formed at a spreading center in early Ordovician time and obducted or uplifted between middle Ordovician and early Devonian time (Lindsley-Griffith, 1977, 1982). It may underlie the entire Eastern Klamath Subprovince as a gently dipping sheet like mass (Irwin, 1977).

Overlying the Trinity Ophiolite are Paleozoic and Mesozoic sedimentary and volcanic rocks of varying metamorphic grade. These rocks are separated into the Yreka-Callahan terrain in the northwest, and the Redding terrain in the southeast by a large exposure of the underlying Trinity Ophiolite (Figure 5). The rocks of the Redding and Yreka-Callahan terrains have been subdivided into the formational units shown in Figure 6.

The rocks of the Yreka-Callahan terrain were originally divided into the Ordovician Duzel Formation and the Silurian Gazelle Formation by Wells et al. (1959). More recent work, summarized by Potter et al. (1977) and Lindsley-Griffith (1982), has revealed complicated structural and stratigraphic relations within and between these formations. Furthermore, portions of the Duzel are
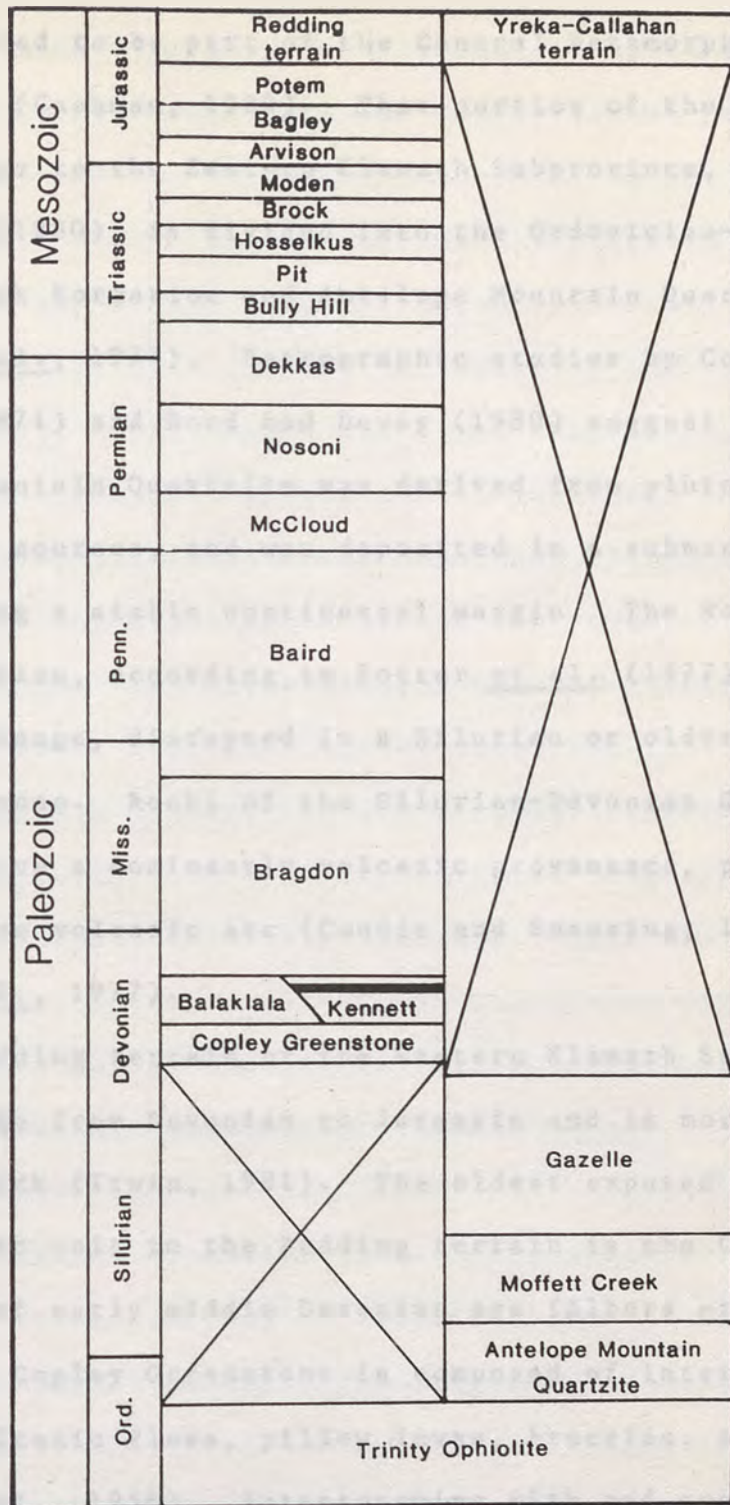
Figure 6 Stratigraphy of the Eastern Klamath Subprovince.
Heavy line shows position of Glidden bedded barite.
After Irwin (1981).

now considered to be part of the Central Metamorphic Belt
to the west (Cashman, 1980). That portion of the Duzel
which belongs to the Eastern Klamath Subprovince, according
to Cashman (1980), is divided into the Ordovician-Silurian
Moffett Creek Formation and Antelope Mountain Quartzite
(Potter et al., 1977). Petrographic studies by Condie and
Snansing (1971) and Bond and Devay (1980) suggest that the
Antelope Mountain Quartzite was derived from plutonic-
metamorphic sources, and was deposited in a submarine fan
complex along a stable continental margin. The Moffett
Creek Formation, according to Potter et al. (1977), is a
tectonic melange, disrupted in a Silurian or older
subduction zone. Rocks of the Silurian-Devonian Gazelle
Formation have a dominantly volcanic provenance, possibly a
calc-alkaline volcanic arc (Condie and Snansing, 1971;
Potter et al., 1977).

The Redding terrain of the Eastern Klamath Subprovince
ranges in age from Devonian to Jurassic and is more than
10,000 m thick (Irwin, 1981). The oldest exposed
stratigraphic unit in the Redding terrain is the Copley
Greenstone of early middle Devonian age (Albers et al.,
1981). The Copley Greenstone is composed of intermediate
to mafic volcanic flows, pillow lavas, breccias, and tuffs
(Kinkle et al., 1956). Intertonguing with and overlying
the Copley Greenstone is the Balaklala Rhyolite which
consists of rhyolite flows, pyroclastics, and shallow

intrusives (Kinkle et al., 1956; Irwin, 1977). Murray and
Condie (1973) have found that the Copley-Balaklala sequence
is chemically similar to recent calc-alkaline arc sequences
of the Pacific area. The widespread distribution of the
Copley-Balaklala sequence, first noted by Hershey (1901)
and Hinds (1932), is suggestive of multiple source areas
(Kinkle et al., 1956; Albers and Robertson, 1961).

Conformably overlying the Copley-Balaklala sequence is
the middle Devonian (Diller and Schuchert, 1894; Savage,
1976) Kennett Formation which is the host rock at the
Glidden deposit. The discontinuous Kennett Formation is
composed of black siliceous shale, rhyolitic tuff, and
limestone (Kinkle et al., 1956). At some locations the
Kennett is missing, and the Mississippian Bragdon Formation
overlies the Copley-Balaklala sequence. This has been
interpreted to be the result of non deposition and abrupt
facies changes due to topographic irregularities in a
volcanic island arc environment (Kinkle et al., 1956;
Albers and Robertson, 1961).

Overlying the Kennett Formation are volcanic and
sedimentary rocks composed of three volcanic phases
separated by limestone units (Murray and Condie, 1973).
The episodes of increased volcanism are represented by the
Carboniferous Bragdon and Baird Formations, the Permo-
Triassic Nosoni, Dekkas, and Bully Hill Formations, and the
late Triassic and Jurassic Modin, Arvison, Bagley, and

Potem Formations (Murray and Condie, 1973). The limestone units separating these volcanic phases are the Permian McCloud and Triassic Hosselkus Formations (Murray and Condie, 1973).

Correlations

Diller (1892, 1906) was one of the first geologists to recognize the similarity between rocks of the Eastern Klamath Subprovince and those of the northern Sierras. More recently, petrographic and paleontologic studies have provided some evidence to support Diller's original proposal (Bond and Devay, 1980; Boucot et al., 1974).

Basement rocks in the Eastern Klamath Subprovince are interpreted to be an ophiolite sequence (Lindsley-Griffith, 1977). Ultramafic rocks along the Melones fault zone in the northern Sierras may also represent an ophiolite (Moores, 1970) correlative with the Trinity Ophiolite of the eastern Klamaths (Davis, 1969). Bond and Devay (1980) concluded from petrographic studies that the Antelope Mountain Quartzite in the eastern Klamaths and quartzose sandstones of the "lower" Shoo Fly in the northern Sierras, although not necessarily contemporaneous, are probably lithologic equivalents. The discontinuous distribution of the Kennett Formation in the eastern Klamaths and of the "upper" Shoo Fly (Sierra Buttes?, Grizzly?) in the northern Sierras is the result of locally restricted deposition

controlled by irregular topography in a volcanic arc environment (Kinkle et al., 1956; Albers and Robertson, 1961; McMath, 1966). Although the Kennett Formation and the "upper" Shoo Fly may have been deposited in similar geologic settings, their stratigraphic relationships to major accumulations of island arc volcanics are different. The Kennett Formation was deposited during the waning stages of arc volcanism (i.e. post Copley-Balaklala), while the "upper" Shoo Fly was deposited during the initial stages of arc volcanism (i.e. pre-Taylor). However, because arc volcanism started somewhat earlier in the eastern Klamaths than in the northern Sierras (Potter et al., 1977; D'Allura et al., 1977) it is possible that the subject deposits are somewhat contemporaneous. Davis (1969) correlated major thrust faults in the Klamath Mountains (Trinity thrust fault) with steeply dipping faults of the northern Sierras (Melones fault zone), and Boucot et al. (1974) present evidence for a widespread middle Devonian unconformity affecting the eastern Klamaths and the northern Sierras.

Correlations between Paleozoic rocks of the eastern Klamaths-northern Sierras and those of north central Nevada are more tenuous. Many authors have noted lithologic, stratigraphic, and tectonic similarities between Paleozoic rocks of the eastern Klamath-northern Sierra region and rocks of the "Antler allochthon" (D'Allura et al., 1977;

Irwin, 1977; Bond and Devay, 1980; Schweickert and Snyder, 1981; Girty, 1983). Although positive correlations have not been documented these similarities may be evidence of Paleozoic continuity between these areas. The presence of bedded barite in Paleozoic rocks of all three regions is entirely consistent with this interpretation. The stratigraphic positions of some mid-Paleozoic bedded barite bearing rocks of the eastern Klamaths, the northern Sierras, and north central Nevada are shown in Figure 7. It is interesting to observe that the bedded barite occurs in progressively younger rocks in a roughly west to east direction. Since the Glidden and Almanor deposits are associated with rocks considered to be volcanic arc deposits, this pattern could be interpreted as eastward migration of a volcanic arc (barium source (?)), culminating in the Devono-Carboniferous Antler Orogeny. Alternatively, the Paleozoic rocks hosting the subject deposits may be remnants of a microplate whose geologic evolution, prior to accretion during Mesozoic time, was unrelated to Paleozoic rocks of north central Nevada (Churkin and Eberlein, 1977; Speed, 1979).

Geologic history

The Paleozoic rocks of the northern Sierras and of the eastern Klamaths share a similar geologic history. In both areas the rocks seem to record a transition from stable

	Klamaths	Sierras	Shoshone Range	Toiyabe Range	Toquima Range	Snake Mts.
Miss.	Bragdon	Peale				Webb
		Taylor				
		Elwell				
Devonian		Sierra Buttes	Slaven Chert	Slaven Chert	Slaven Chert	Slaven Chert
	Kennett Balaklala Copley	"Middle" Shoo Fly				

Figure 7   Stratigraphic position of some bedded barite deposits in the western United States. Heavy lines represent bedded barite. After Poole et al. (1977) and Poole et al. (1981).

continental margin conditions ("lower" Shoo Fly and
Antelope Mountain Quartzite) to a volcanic arc type
environment (Sierra Buttes and Copley-Balaklala).
Associated with this transition are subduction related
melange units ("middle" Shoo Fly and Moffett Creek
Formation). This Klamath-Sierran volcanic arc persisted
with only minor interruption throughout late Paleozoic time
(Murray and Condie, 1973; D'Allura et al, 1977).

GEOLOGY OF THE BARITE DEPOSITS

Almanor Deposit

Bedded barite at the Almanor deposit is
discontinuously exposed in road cuts and mine workings for
approximately 1 km in a northwest-southeast trend along the
eastern overturned limb of the northwest plunging Almanor
anticline (Figures 3 and 8).

The oldest exposed stratigraphic unit in the area of
Figure 8 is the uppermost part of the Eocambrian (?) to
Devonian (?) Shoo Fly complex. At the Almanor deposit the
"upper" Shoo Fly is composed of light gray to black chert,
siliceous shale-argillite, bedded barite, and lenticular
bodies of quartzite. D'Allura et al. (1977) also observed
tuff lenses and relic pumice shards indicating a volcanic
source for many of the "upper" Shoo Fly rocks. The
structural and stratigraphic relationship between the
undated "upper" Shoo Fly and the older "middle" Shoo Fly of
probable Ordovician-Silurian age (Varga and Moores, 1981)
is not clear. D'Allura et al. (1977) suggest that they may
be unconformable; however, this contact is poorly exposed
in the vicinity of the Almanor deposit. Varga (1980)
documents two periods of folding and deformation in Shoo
Fly rocks south of the study area. An earlier pre-Nevadan
deformation is apparently confined to Shoo Fly rocks,
whereas the younger Nevadan deformation has affected both
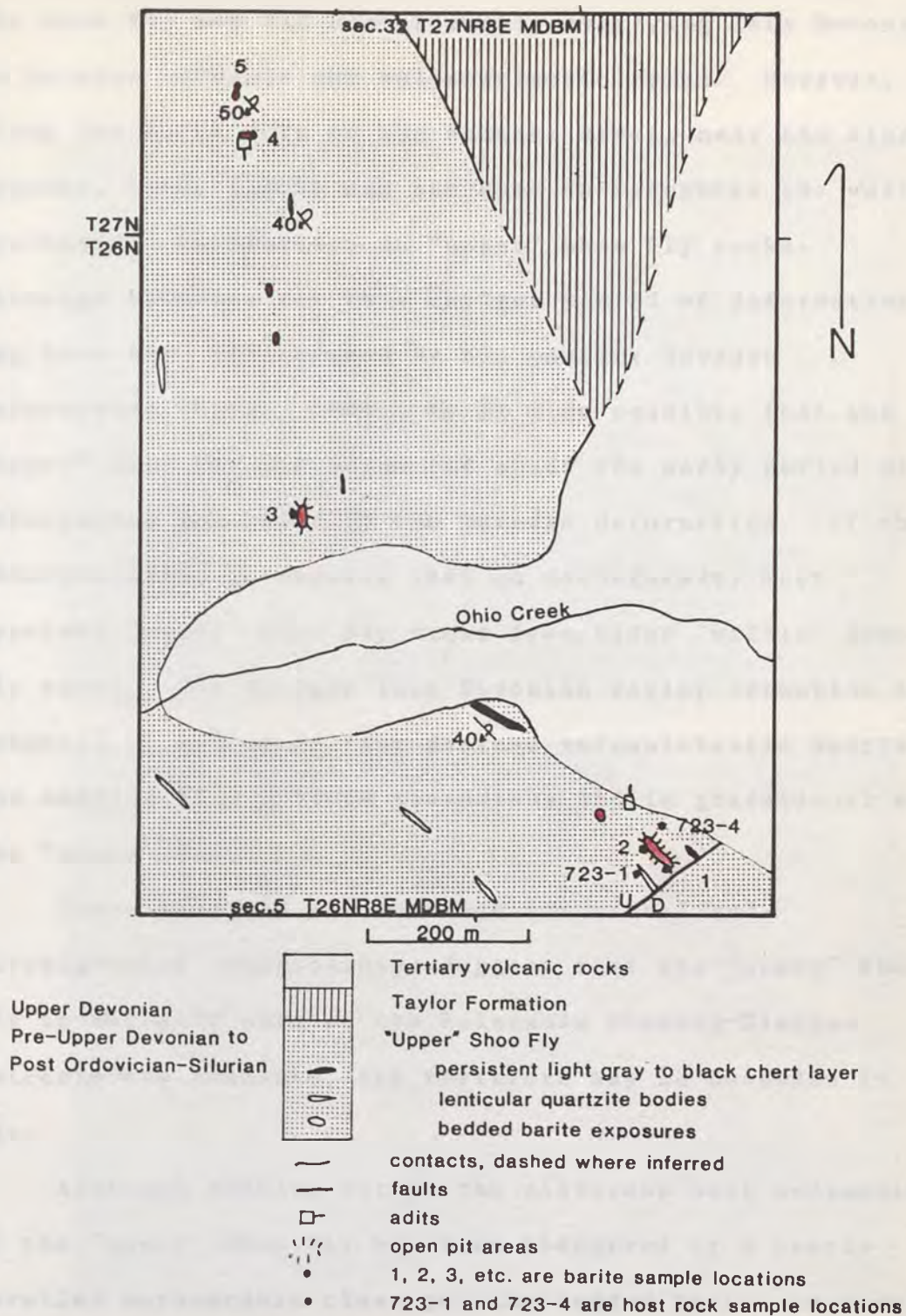
Figure 8 Geologic map of the Almanor bedded barite deposit.

the Shoo Fly and the unconformably overlying late Devonian to Permian volcanic and volcaniclastic rocks. However, along the North Fork of the Feather River, near the Almanor deposit, Varga (1980) was not able to recognize the earlier pre-Nevadan deformation in "upper" Shoo Fly rocks. Although evidence for this earlier period of deformation may have been obliterated by the younger Nevadan deformation (Varga, 1980), it is also possible that the "upper" Shoo Fly was deposited after the early period of deformation but prior to the Nevadan deformation. If this interpretation is correct then an unconformity must separate "upper" Shoo Fly rocks from older "middle" Shoo Fly rocks. The younger late Devonian Taylor formation is composed of medium to fine grained volcaniclastic debris and massive fine grained greenstone and is gradational with the "upper" Shoo Fly.

These inferred and observed structural and stratigraphic relationships suggest that the "upper" Shoo Fly is actually part of the Paleozoic Klamath-Sierran volcanic arc sequence, and therefore may be Devonian in age.

Although bedding within the siliceous host sediments of the "upper" Shoo Fly has been obscurred by a nearly parallel metamorphic cleavage, the bedded barite is clearly conformable, at map and outcrop scales, to adjacent lithologically distinct sedimentary units (Figures 8 and

Figure 9   Photographs of bedded barite exposures, Almanor deposit.
Barite layers are marked "Ba"; host rocks are marked "H".
Point "P" is common to both photographs.

Sample locations shown on figure 8

1   2   3   4   5

-4

⊙Al-3   Al-6 ⊙

⊙Al-9

-3
⊙Al-8
Al-10

fault zone   ⊙Al-2   Al-5 ⊙

-2

meters

⊙Al-7

-1

⊙Al-1   Al-4 ⊙

-0
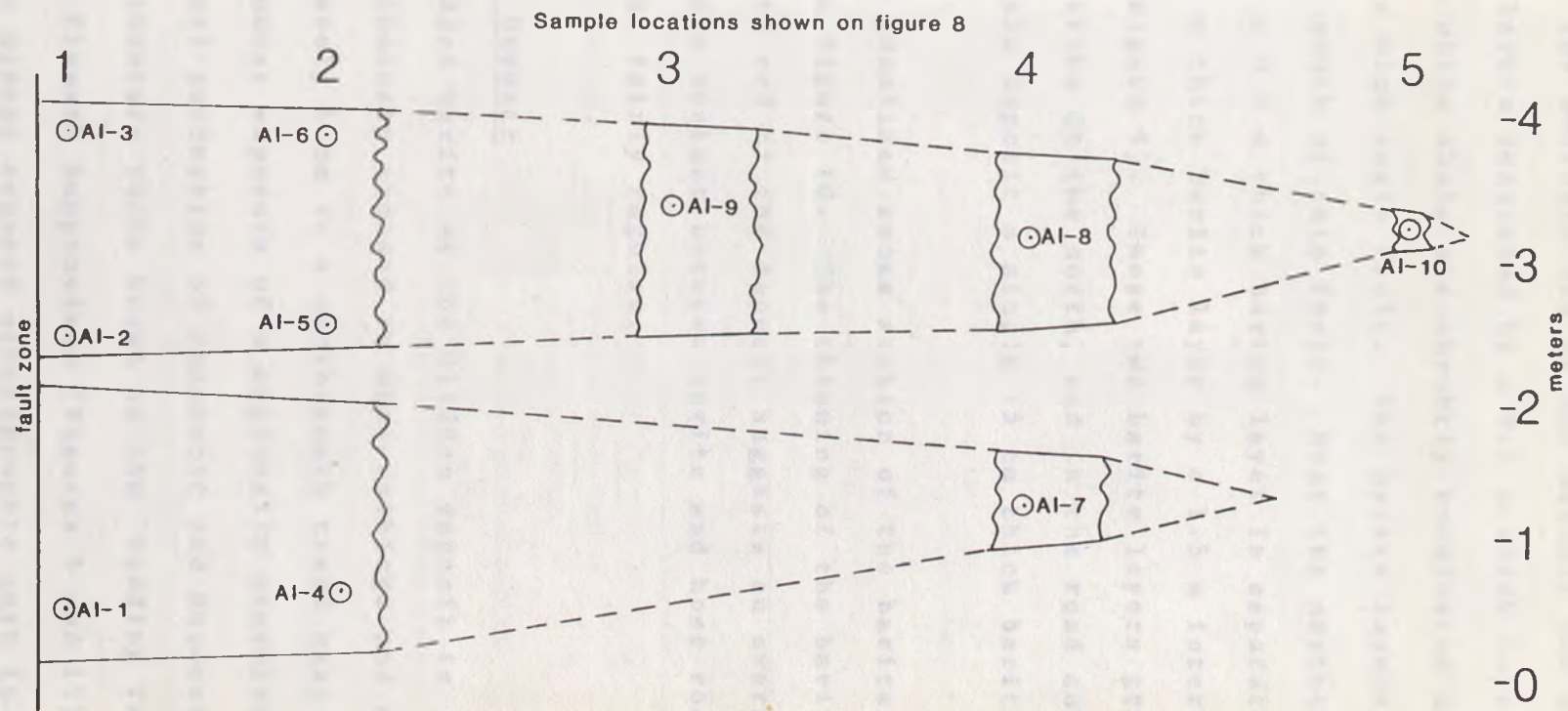
Figure 10   Idealized cross-section of the Almanor barite deposit.
Al-1,2.... are sample locations.

9). At the southern end of the deposit two 2 m thick barite layers separated by a 0.2 m thick layer of light gray to white shale are abrubtly terminated by an east-west striking high angle fault. The barite layers are not exposed south of this fault. Near the northern end of the deposit a 0.5 m thick barite layer is separated from a 1.0 m - 1.5 m thick barite layer by a 1.5 m interval of brown shale (Figure 9). These two barite layers gradually narrow along strike to the north, and in the road cut at the north end of the deposit a single 15 cm thick barite layer is exposed.

An idealized cross section of the barite ore zone is shown in Figure 10. The thinning of the barite layers at the north end of the deposit suggests an overall lenticular form. The contact between barite and host rock is usually sharp and fairly regular.

Glidden Deposit

Bedded barite at the Glidden deposit is discontinuously exposed in mine workings and outcrop for approxmately 1 km in a north-south trend near the northernmost exposure of a regionally southeast dipping homoclinal succession of Paleozoic and Mesozoic volcanic and sedimentary rocks known as the "Redding Terrain" of the Eastern Klamath Subprovince (Figures 5 and 11).

The oldest exposed stratigraphic unit in the area of
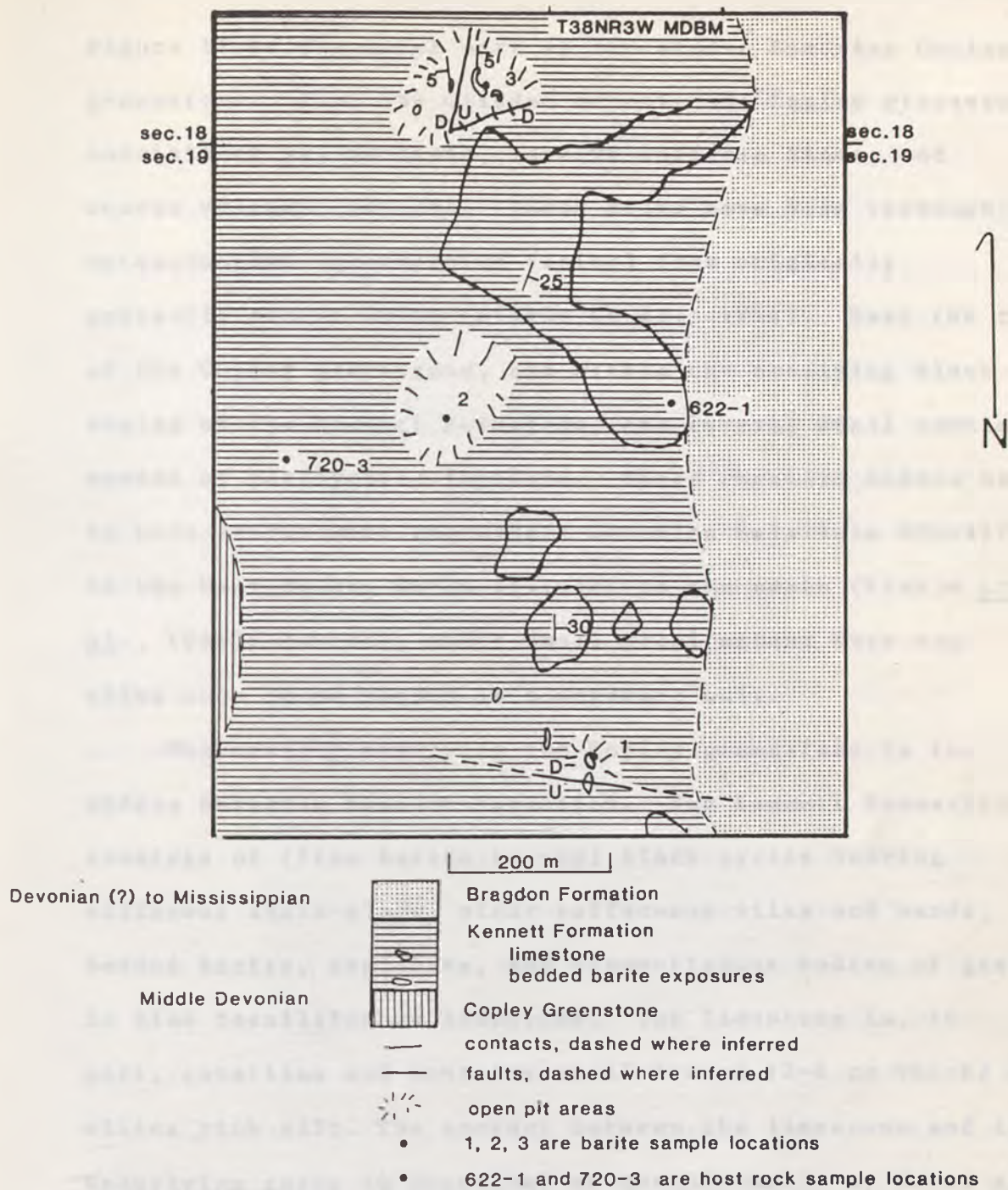
Figure 11 Geologic map of the Glidden bedded barite deposit.
After Weber and Matthews (1967).

Figure 11 is the upper part of the middle Devonian Copley greenstone. Near the Glidden deposit the Copley greenstone consists of pillow lavas, massive volcanic flows, and coarse volcanic breccia. These rocks have been thoroughly metamorphosed (greenschist facies) from originally andesitic parent rocks (Kinkle et al., 1956). Near the top of the Copley greenstone, and within the overlying black shales of the Kennett Formation, are several small tabular masses of porphyritic rhyolite. These rhyolite bodies may be correlative with the middle Devonian Balaklala Rhyolite in the West Shasta Cu-Zn district to the south (Kinkle et al., 1956); however, their small areal extent does not allow them to be mapped as a separate unit.

Conformably overlying the Copley greenstone is the middle Devonian Kennett Formation. The Kennett Formation consists of (from bottom to top) black pyrite bearing siliceous shale-slate, minor tuffaceous silts and sands, bedded barite, argillite, and discontinuous bodies of gray to blue fossiliferous limestone. The limestone is, in part, coralline and contains small lenses (2-4 cm thick) of silica rich silt. The contact between the limestone and the underlying rocks is described as unconformable by Weber and Matthews (1967). However, the lower part of the limestone is brecciated in places and the subadjacent shale-argillite has been sheared and folded; possibly the result of gravitational sliding of reef deposits into deeper water

muds. Overlying the Kennett Formation is the late Devonian (?) to Mississippian Bragdon Formation. The contact between the Kennett and Bragdon Formations has been variously described as conformable (Kinkle et al., 1956), to "probably unconformable" (Irwin, 1977). Since this contact is defined by the top of the limestone layer in the Kennett Formation (Kinkle et al., 1956) these conflicting interpretations are not surprising; both may be correct. The rocks above the limestone at the Glidden deposit consist of brown to gray shales and siltstones, and are similar to the rocks beneath the limestone.

The barite layers at the Glidden deposit are distinctly bedded and are conformable with the host sediments (Figure 12). Sedimentary features within the barite layers include lens like structures and laminae (Figure 13). At the northern end of the deposit a lower 1.0 to 1.5 m thick layer of massive fine grained black barite is separated from an upper 0.5 to 1.0 m thick layer of gray to brown laminated barite and interlaminated barite and silica by a 2 m thick interval of gray argillite. In some exposures the upper laminated barite bed is separated into two similar layers by a 10-20 cm thick lens of siltstone. A similar sequence, consisting of a 1.5 m thick lower massive barite bed and an upper 2 m thick laminated barite bed, is exposed near the south end of the deposit. Contacts between barite and host vary from sharp to

Figure 12   Photograph of bedded barite exposure, Glidden deposit.
            Bottom of barite layer is at the top of the hammer and
            extends to the top of the photograph.

Figure 13 Photographs of sedimentary features in bedded barite from
the Glidden deposit. Top: lens like structure in laminated
barite and quartz; bottom: barite laminae.

gradational and are usually regular. An idealized cross section of the barite ore zone is shown in Figure 14.

The attitude of the barite beds and host sediments changes from relatively flat lying in the north to moderately east dipping in the south, suggesting a small monoclinal "warp" in the regionally southeast dipping sediments. Minor high angle faults have affected the barite beds and host sediments near the Glidden deposit. These faults are marked by fissure filling quartz veins in host rock lithologies and clear to white fissure filling vein barite plus or minus quartz in the barite interval. Displacement along these faults is minor (2-3 m).

Sedimentary clasts of sulfides, probably derived from the West Shasta volcanogenic massive sulfide ores (Watkins and Stensrud, 1983), are present in rocks of the Kennett Formation at exposures near the Glidden deposit. The stratigraphic position of these clasts is equivalent to the limestone unit in the upper part of the Kennett Formation (Watkins and Stensrud, 1983). Since this limestone unit is stratigraphically above the barite beds at the Glidden deposit it is possible that the massive sulfide ores of the West Shasta District and the bedded barite of the Glidden deposit are contemporaneous.
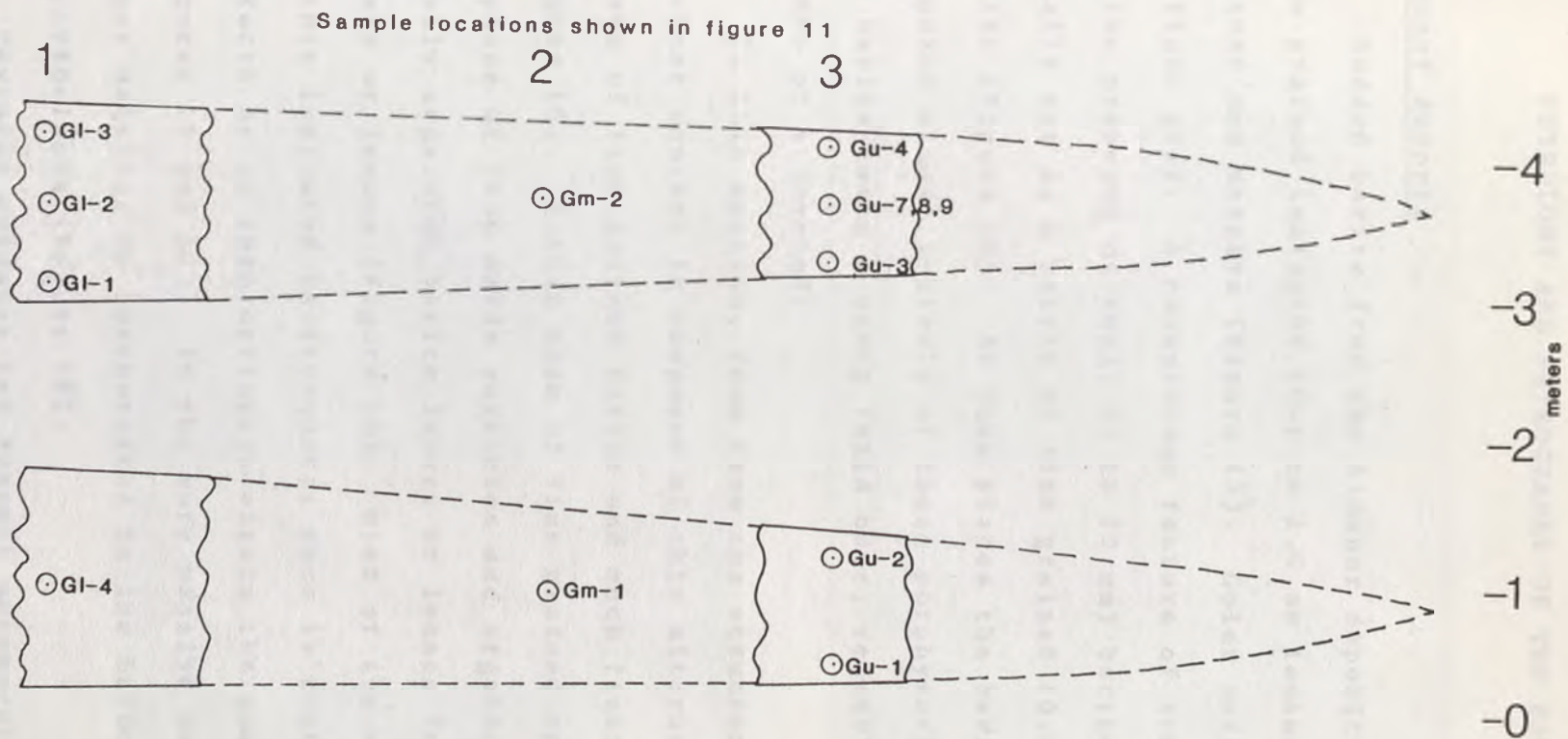
Figure 14   Idealized cross-section of the Glidden deposit.   Gu-1,2.... are sample locations.

PETROLOGY AND PETROGRAPHY OF THE BARITE ORES

Almanor deposit

Bedded barite from the Almanor deposit ranges from
fine grained laminated (0.1 to 1.0 mm laminae) to coarse
grained and massive (Figure 15). Color varies from black
to light gray. A conspicuous feature of some of the barite
is the presence of small (2 to 10 mm) barite porphyroclasts
usually set in a matrix of fine grained (0.05 to 0.10 mm)
barite (Figure 15). At some places the barite rock is
composed almost entirely of these porphyroclasts. All of
the barite emits a stong fetid odor, resembling H_2S, when
broken or scratched.

In thin section, rock from the structurally higher
ore-host contact is composed of thin alternating layers or
lenses of fine grained barite and much finer grained quartz
(Figure 16). A thin seam of fine grained opaque material,
composed of iron oxide particles and organic (?) debris,
usually separates barite layers or lenses from quartz
layers or lenses (Figure 16). Most of the opaque material
in this laminated barite-quartz rock is confined to these
contacts or to thin stringers within the quartz layers
(Figures 16 and 17). In the more massive barite, the
opaque material is concentrated in the barite
porphyroclasts (Figure 18).

Textural evidence for dynamic metamorphism is apparent

Figure 15   Photographs of barite samples, Almanor deposit.   Top:
            laminated barite, note porphyroclasts of barite; bottom:
            massive barite.

Figure 16   Photomicrographs of interlaminated barite and quartz, Almanor
deposit. The coarser grained material is barite. The black
seams are composed of iron oxide particles and organic (?)
material. Top: crossed polars; bottom: plane polarized light.
Bars are 1 mm long.
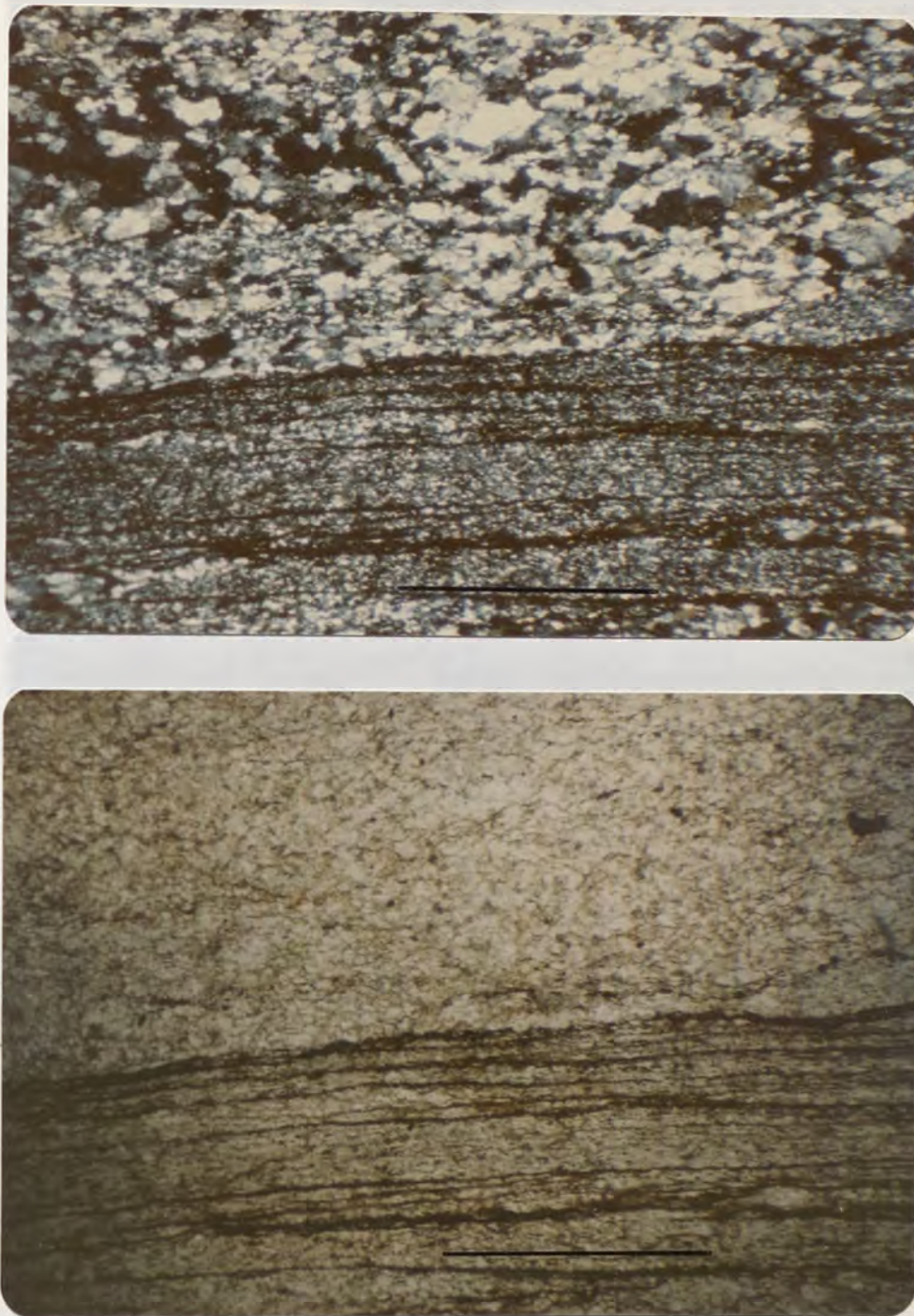
Figure 17 Photomicrographs of laminated barite and quartz, Almanor
deposit. The coarser grained material at the top of both
photographs is barite. The black seams are composed of
iron oxide particles and organic (?) material. Top: crossed
polars; bottom: plane polarized light. Bars are 1 mm long.
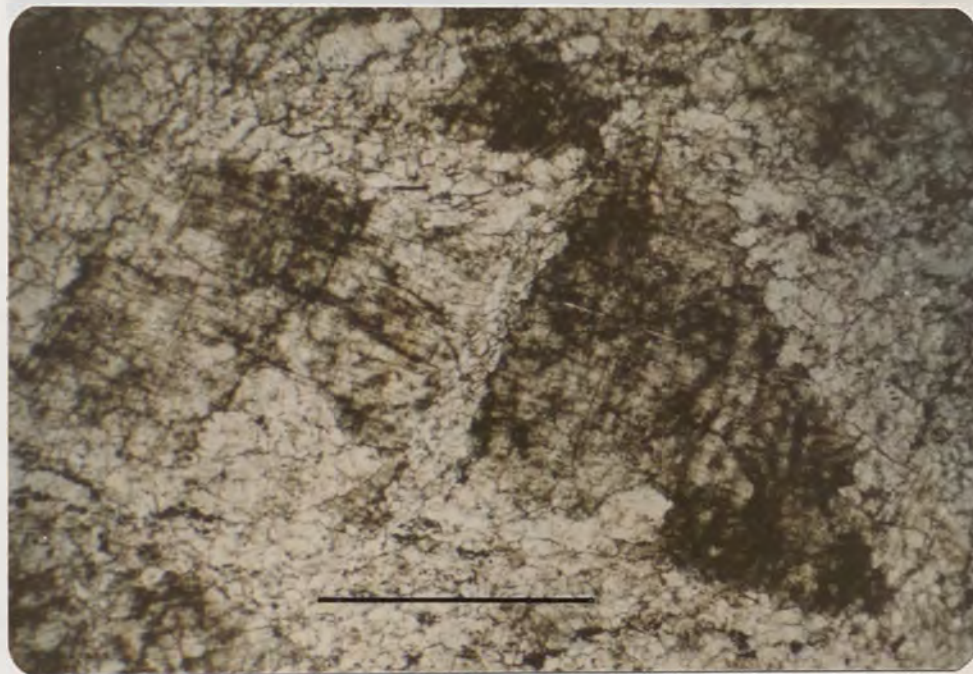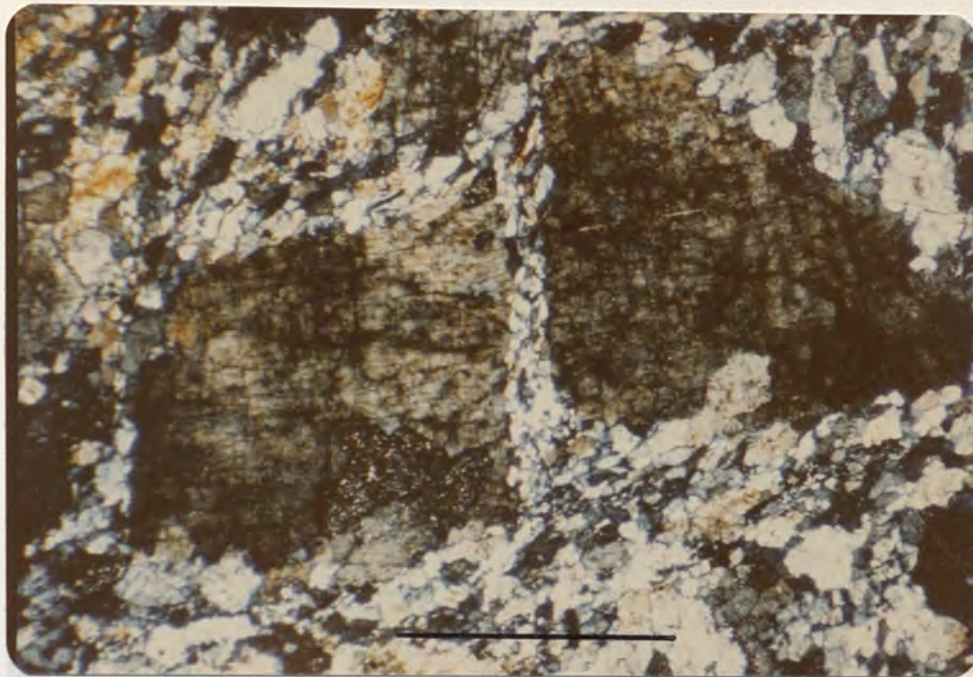
Figure 18 Photomicrographs of a sheared barite porphyroclast set in a matrix of fine grained barite, Almanor deposit. The black material within the porphyroclast is composed of iron oxide particles and organic (?) material. Top: crossed polars; bottom: plane polarized light. Bars are 1 mm long. (Note: bottom photograph is rotated approximately 25 degrees clockwise)
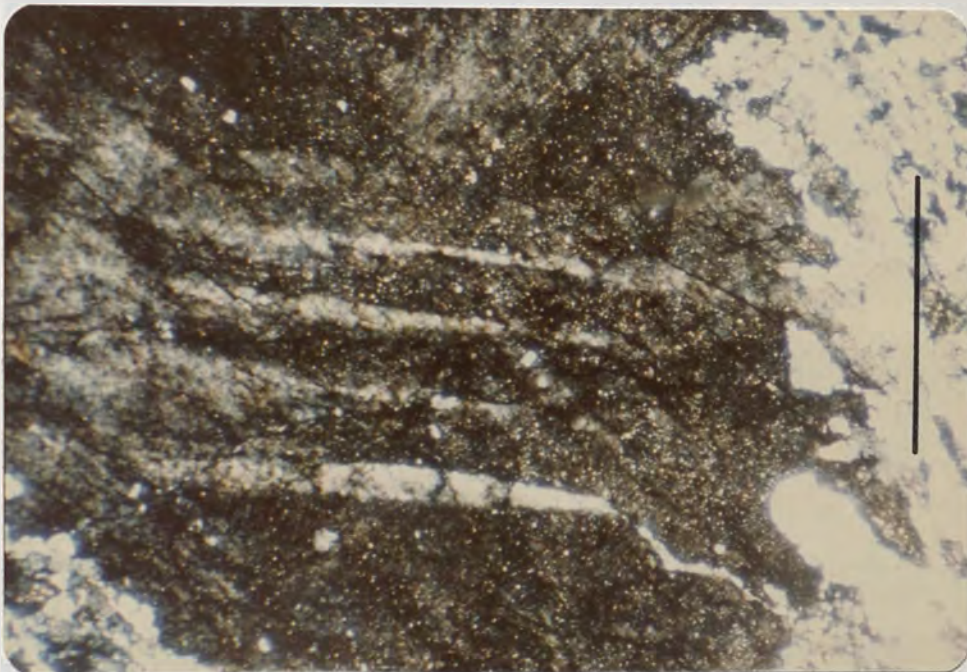
Figure 19 Photomicrograph showing tapering deformation bands in barite porphyroclast, Almanor deposit. (c.f. Tieman and Kopp, 1983, Figure 4). Note numerous inclusions in the darker areas of photograph. Crossed polars. Bar is 1 mm long.
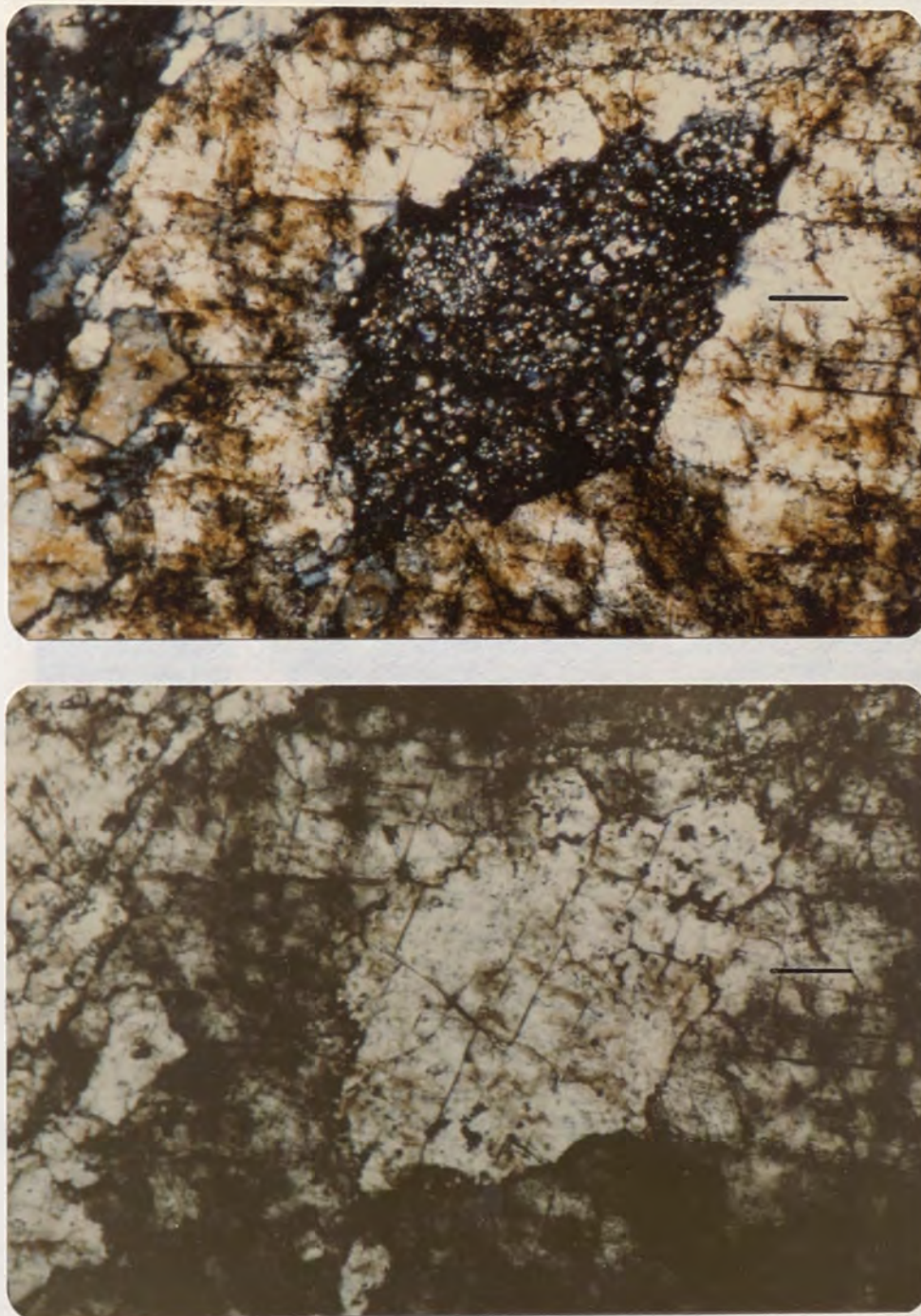
Figure 20 Photomicrographs showing recrystallized portion of barite
porphyroclast, Almanor deposit. Organic (?) material that
has been rejected from the recrystallized area is concentrated
in a thin seam outlining that area (bottom photograph).
Note numerous birefringent inclusions. Top: crossed polars;
bottom: plane polarized light. Bars are 1 mm long.
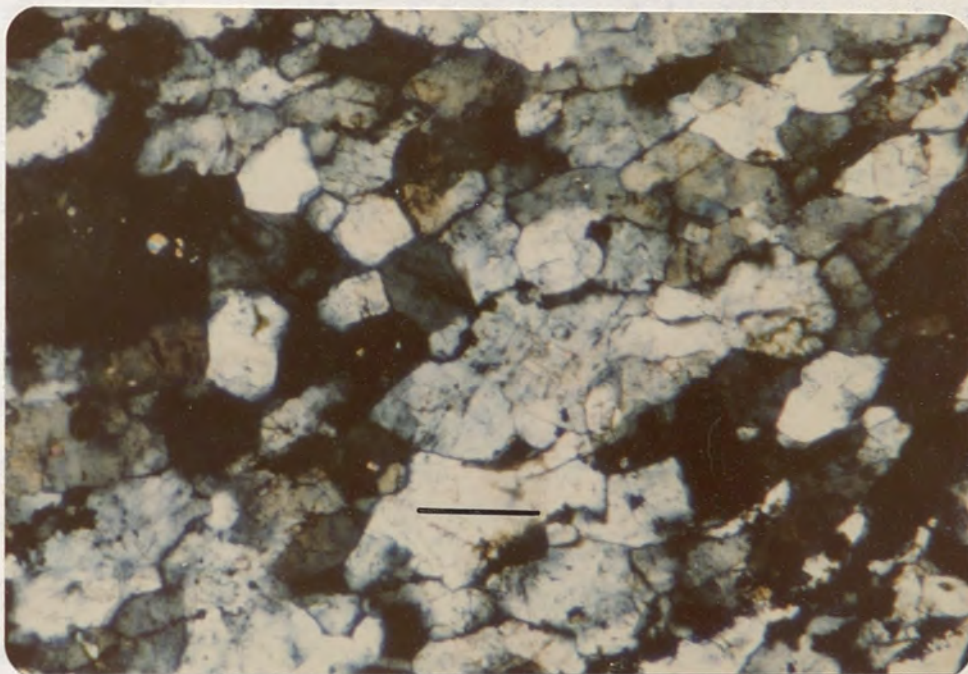
Figure 21   Photomicrograph showing polygonal mosaic of barite crystals, Almanor deposit. Note triple points. Crossed polars. Bar is 1 mm long.

in barite from the Almanor deposit. Deformation fabrics,
including deformation bands (Figure 19), and sheared and
partly recrystallized barite porphyroclasts (Figures 18 and
20) can be recognized. The high concentration of opaque
organic (?) material trapped in these porphyroclasts makes
them easily visible in plane polarized light (Figure 18).
In some samples, a polygonal mosaic of barite crystals has
developed (Figure 21), suggesting that recrystallization
has also occurred without accompanying stress. Numerous
inclusions of birefringent minerals produce a sieve texture
in many barite grains and porphyroclasts (Figures 19 and
20). Many of these mineral inclusions exhibit bright
second and third order interference colors (Figures 20 and
21) and have indices of refraction that bracket the indices
of refraction of barite (n = 1.636 - 1.648). The fairly
high interference colors of these mineral inclusions
suggests a carbonate mineral. The low calcium content of
the barite rock (Table 1) and the fetid odor of H_2S may
indicate that these inclusions are witherite produced as a
result of the bacterial reduction of sulfate. The
following chemical reaction, modified from Friedman and
Sanders (1978), explains this process:

$$BaSO_4 + 2CH_2O \longrightarrow BaCO_3 + H_2O + CO_2 + H_2S$$
$$\text{(organics)}$$
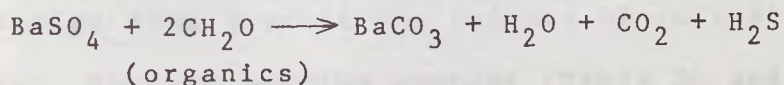
Glidden deposit

Bedded barite from the Glidden deposit also ranges from laminated to massive (Figure 22), however, both types are fine grained (0.05 to 0.15 mm). The laminated barite is usually light brown to light gray and the massive barite ranges from gray to black (Figure 22). At some places the laminated barite is folded and the barite layers thicken in the hinge areas and thin on the limbs (Figure 23). Both laminated and massive barite emit a fetid odor when broken or scratched.

In thin section, the laminated barite is very similar to the laminated barite from the Almanor deposit (Figure 24). Fine grained barite layers or lenses are usually separated from quartz layers or lenses by thin seams of fine grained iron oxide particles and organic (?) material (Figure 24). The massive barite is composed of fine grained barite crystals exhibiting sutured grain boundaries and forming a polygonal mosaic (Figure 25). Numerous inclusions of birefringent minerals produce a sieve texture in many barite grains (Figure 26). These inclusions, like those in the Almanor barite, exhibit bright second and third order interference colors, and have indices of refraction that bracket the indices of refraction of barite. The low calcium content (Table 2) and the fetid odor of H_2S suggests that many of these inclusions are witherite.

Figure 22   Photographs of barite samples, Glidden deposit. Top: laminated
            barite and fine grained quartz, light brown and gray laminae
            are barite, dark brown laminae are iron stained quartz silt-
            stone; bottom: massive barite.

Figure 23   Photograph of fold in laminated barite, Glidden deposit.
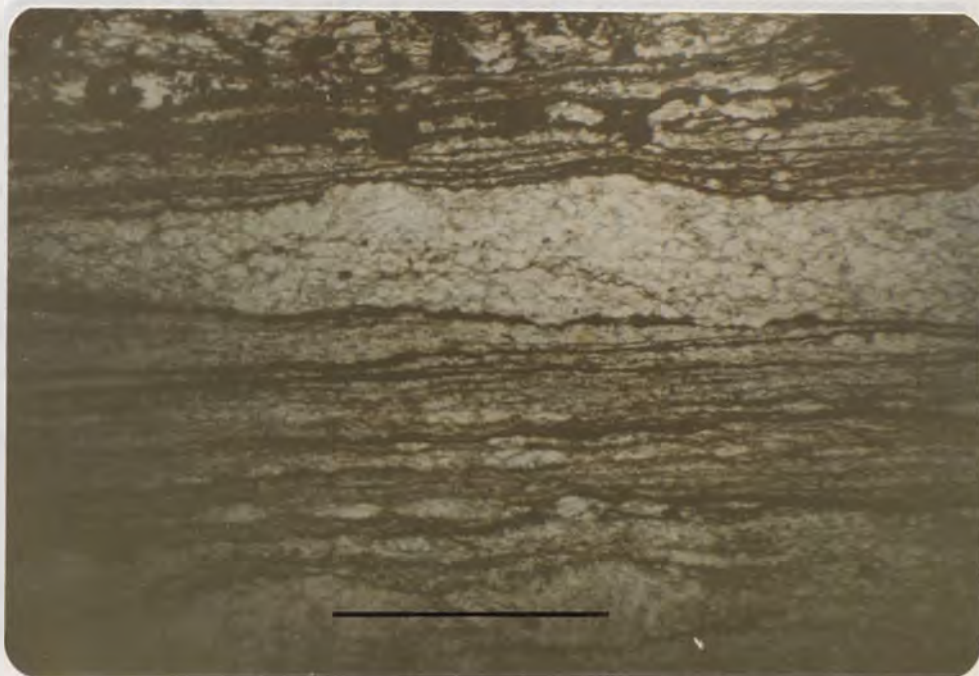Brownish bands are composed of iron stained quartz
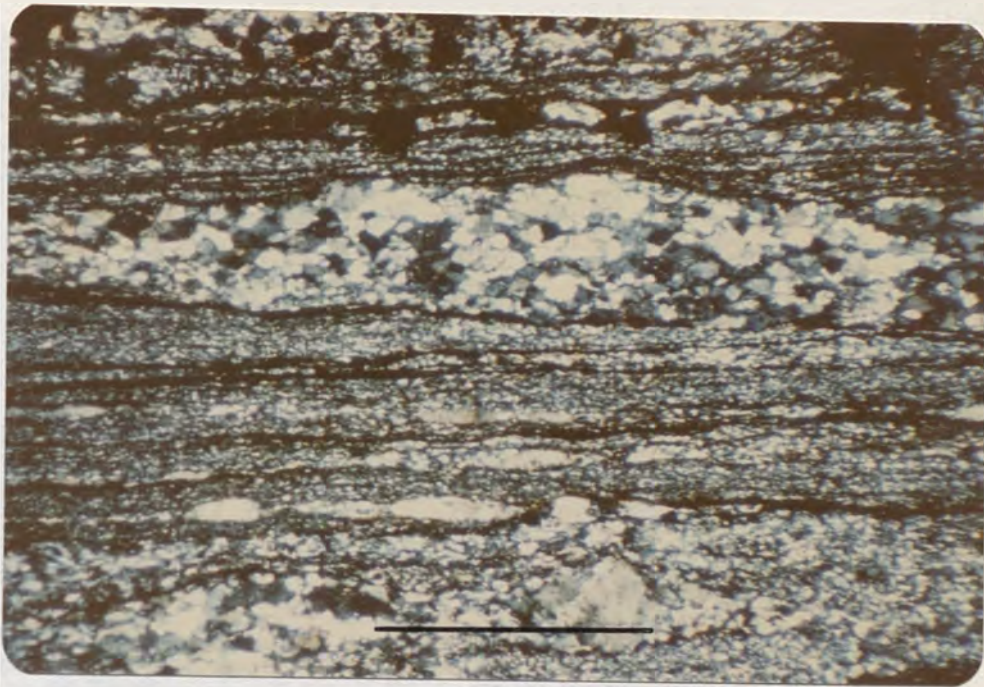siltstone.
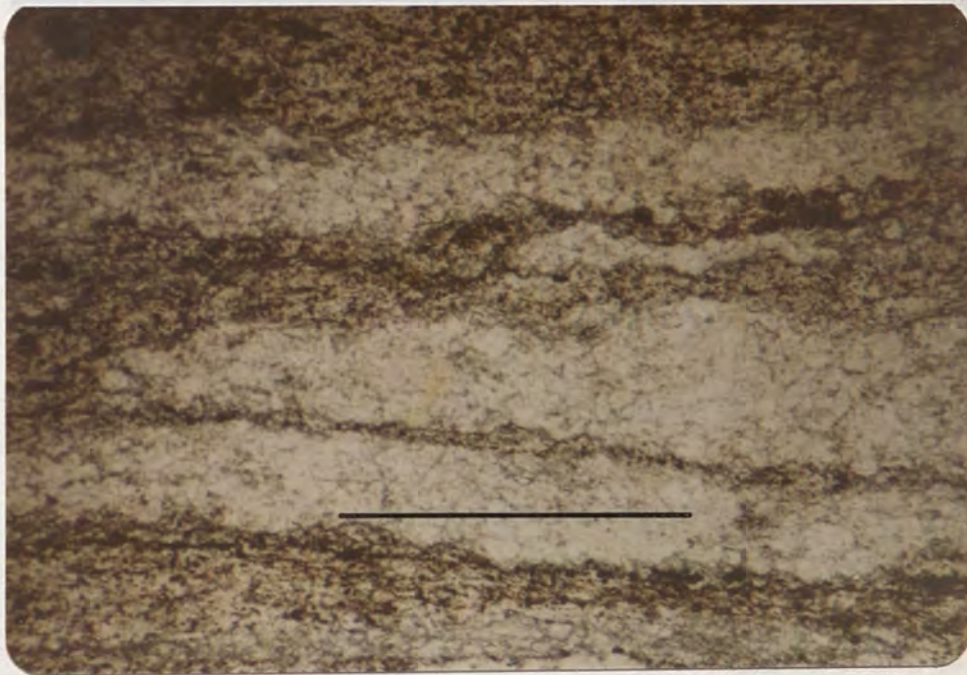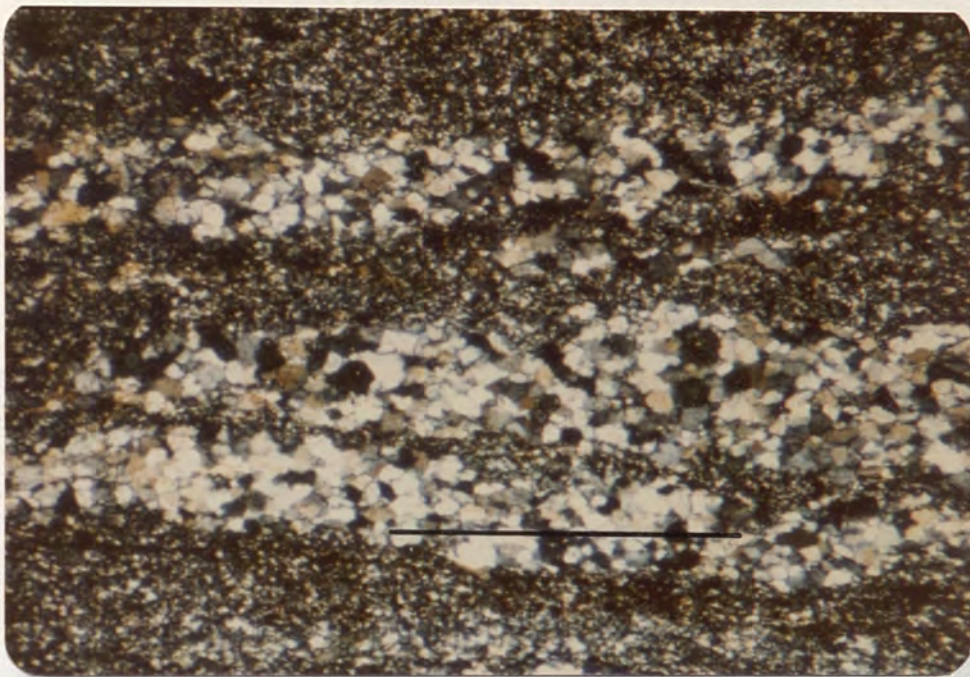
Figure 24 Photomicrographs of interlaminated barite and quartz, Glidden deposit. The coarser grained material is barite. The black material is composed of iron oxide particles and organic (?) material. Top: crossed polars; bottom: plane polarized light. Bar is 1 mm long.
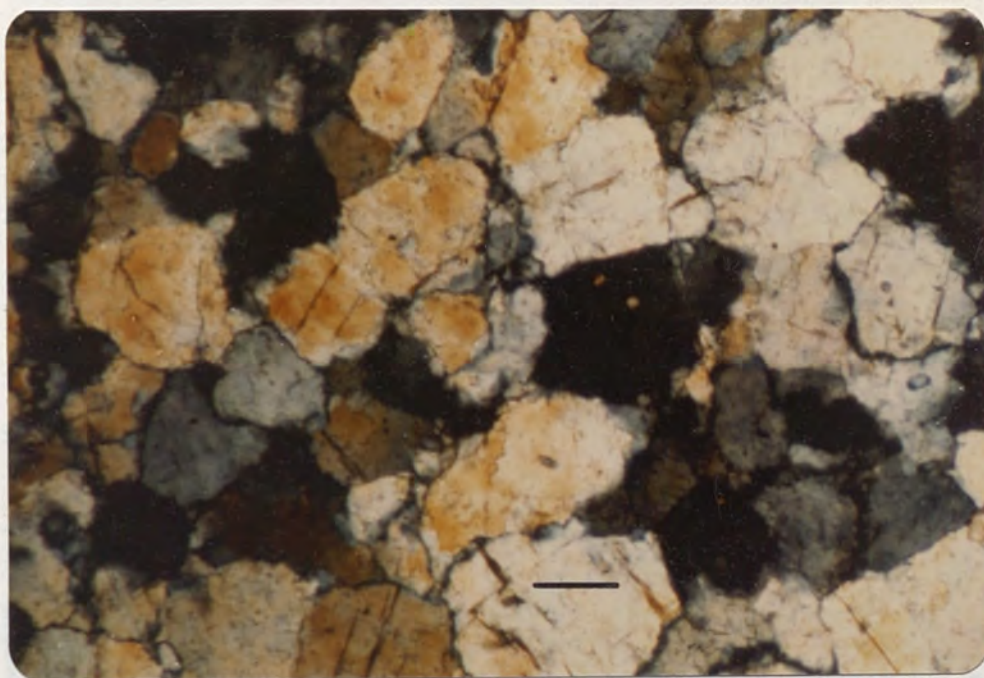
Figure 25   Photomicrograph showing polygonal mosaic of barite crystals,
Glidden deposit. Note sutured grain boundaries and triple
points. Crossed polars. Bar is 1 mm long.
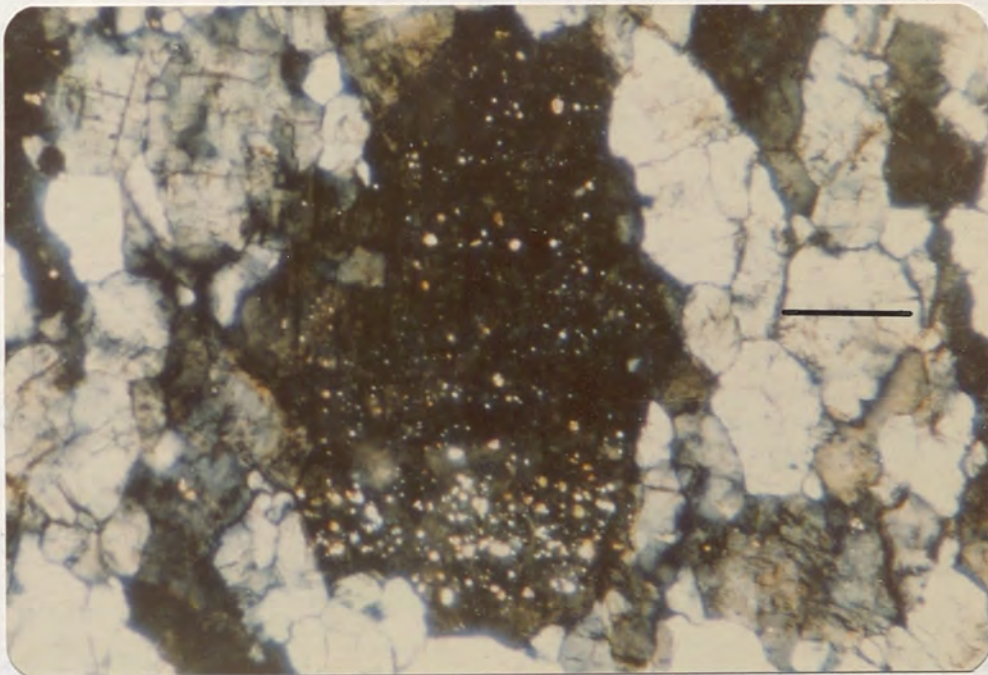
Figure 26 Photomicrograph showing birefringent inclusions in barite
crystal, Glidden deposit. Crossed polars. Bar is 1 mm
long.

Discussion

The folds observed in the laminated barite from the
Glidden deposit suggest that the barite was in place prior
to folding. Similarly, the metamorphic fabrics described
in barite from the Almanor deposit were probably formed
during the Late Jurassic Nevadan orogeny, and thus indicate
that this deposit was in place prior to this time. The
lenticular and layered structure of the laminated barite-
quartz rock of both deposits suggests that the barite was
deposited with the intercalated silica rich sediments.

The consistently coarser grain size of barite over
quartz may be the result of an initially finer grain size
for the quartz layers prior to recrystallization or the
result of continued barite recrystallization under
conditions that did not affect the quartz.

Numerous fluid inclusions can also be seen in thin
sections of barite from the subject deposits. Most of them
are single phase liquid inclusions, but occassionally a
very small vapor bubble is present. Homogenization
temperatures obtained from a doubly polished thin section
of barite from the Almanor deposit ranged from 105° to
115°C. However, the frequently observed recrystallization
textures may indicate that these inclusions were trapped
during recrystallization of the barite.

The numerous barite porphyroclasts observed in barite

from the Almanor deposit may be fragments of pre-existing rosettes or nodules that have been broken and partly recrystallized. Barite rosettes or nodules were not observed at the Glidden deposit.

GEOCHEMISTRY OF THE BARITE

Systematic areal and stratigraphic variations in the minor element content and/or isotopic composition of barite are probably the result of similar variations in the physical and/or chemical environment of mineralization (Hanor, 1966; Rye et al., 1978). Therefore, a knowledge of these variations may prove useful in determining the conditions prevailing during barite deposition. Biologic activity may also leave a unique physical and chemical "imprint" on certain barite occurrences (Miller et al., 1977).

Brobst (1975) observed "that the trace element suite (of bedded barite) is limited, and the abundance of each element is unusually small as compared with the suite and abundance of the trace elements in vein (barite) deposits". He concluded from this observation that bedded barite deposits are probably not of hydrothermal origin (Brobst, 1975).

Sulfur and strontium isotopic studies of widely separated bedded barite deposits have consistently agreed that these elements were most likely derived from contemporaneous seawater (Mitchell, 1977; Rye et al., 1978; Tafuri, 1973; Hulen, 1967; Karunakaran, 1976).

Strontium occurs as a diadochic substitiute for barium in barite, and is the most common minor element found in

barite (Palache et al., 1951; Hanor, 1966). Small scale
variations in the strontium content of barite nodules and
fissure filling crystals have been reported by Hanor (1966,
1969), Clark (1970), Zimmerman (1976), Morrow et al.
(1978), Leach (1980), and Mariano (1980). Deposit wide or
regional zoning of strontium in barite has also been
reported by Zimmerman (1965), Hanor (1966), Tischendorf
(1963), Clark (1970), and Morrow et al. (1978). Many of
these variations have been interpreted to be the result of
the spatial and temporal physico-chemical evolution of the
mineralizing fluids. However, this zoning is not
consistent from deposit to deposit. Some deposits exhibit
an increase in the strontium content of barite with time or
distance from the fluid source area; yet some exhibit
essentially an opposite relation (Hanor, 1966; Tischendorf,
1963, Leach, 1980). In addition, the zoning within some
deposits is cyclic and reversals of the trend of increasing
or decreasing strontium are present (e.g., Figure 32).

Aside from the studies of Heinrich and Vian (1966),
and Mariano (1980), which dealt with the strontium content
of barite from the Mountain Pass, California carbonatite,
there have been no accurate chemical analyses of California
barite.

Sample collection and preparation

A stratigraphically representative suite of barite

samples was collected, in place, from each of the subject deposits. The sample locations are shown in Figures 8, 11, 10 and 14. The strontium content of these samples was determined by x-ray fluorescence spectrometry. In addition, representative samples of bedded and vein barite from several other deposits in California and the neighboring states were also analyzed for strontium. The locations of these additional samples are shown in Figure 27. Several samples of barite and host rocks from the subject deposits were also analyzed by emission spectrography for minor elements other than strontium. The locations of these samples are shown in Figures 8 and 11. Descriptions and other pertinent data regarding all the above samples can be found in the Appendix.

In order to accurately determine the amount of strontium substituting for barium in barite it is necessary to remove any impurities that may contain strontium, or that may introduce errors in the analytic method. Generally, the most abundant impurity in bedded barite is silica, in the form of quartz (Shawe et al., 1969; Brobst, 1975). A substantial density contrast between barite and quartz (4.48 vs. 2.65 g/cc) makes their separation a relatively simple matter using heavy liquids. The following procedure, modified from Volbroth (1963), was used to prepare all samples for x-ray flourescence spectrometry.
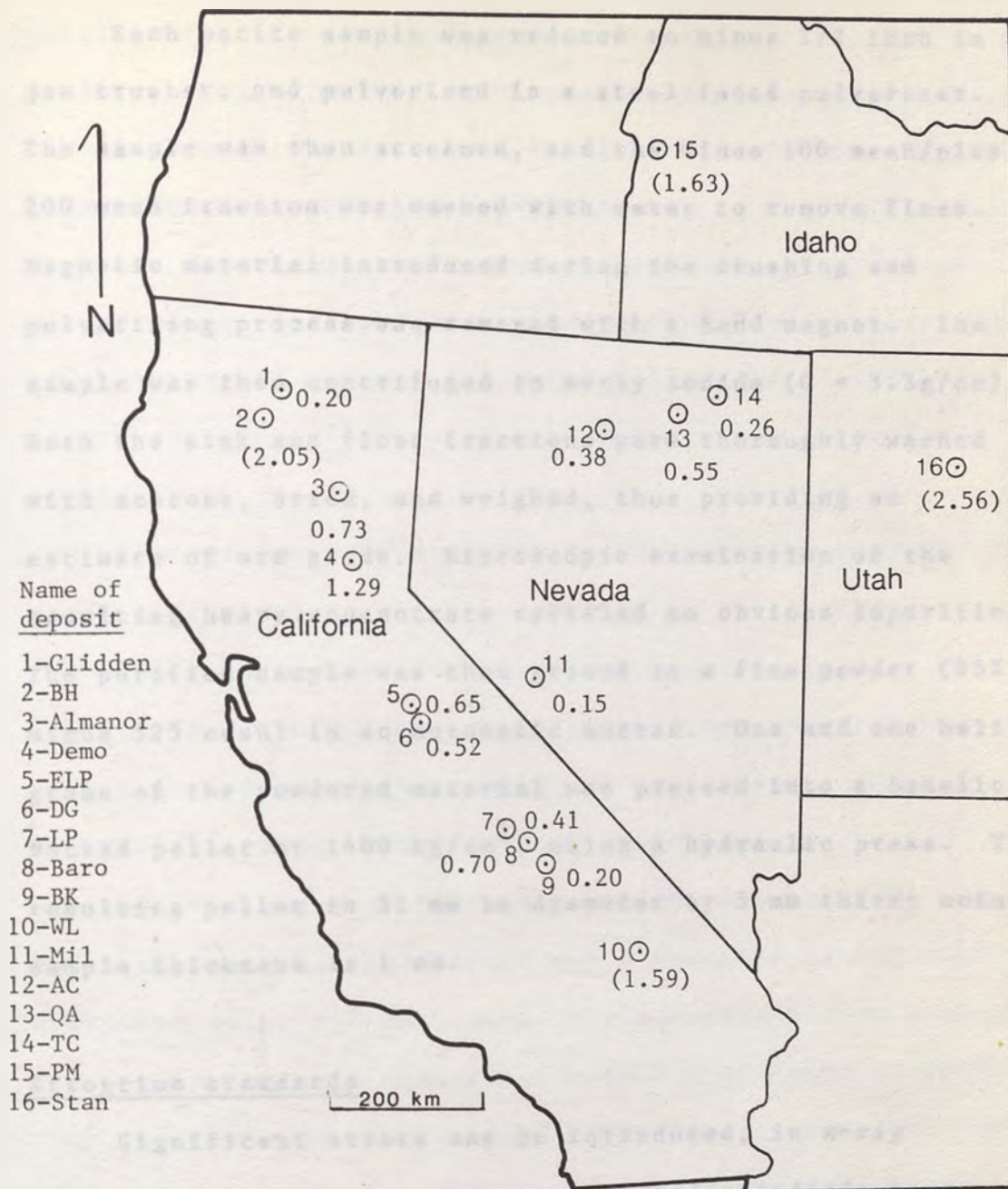
Figure 27   Locations of barite samples analyzed for strontium. Concentrations are mole percent strontium sulfate. Concentrations in brackets are from vein barite or barite associated with volcanogenic massive sulfides, all others are from bedded barite.

Each barite sample was reduced to minus 1/2 inch in a jaw crusher, and pulverized in a steel faced pulverizer. The sample was then screened, and the minus 100 mesh/plus 200 mesh fraction was washed with water to remove fines. Magnetic material introduced during the crushing and pulverizing process was removed with a hand magnet. The sample was then centrifuged in methy iodide (G = 3.3g/cc). Both the sink and float fractions were thoroughly washed with acetone, dried, and weighed, thus providing an estimate of ore grade. Microscopic examination of the resulting heavy concentrate revealed no obvious impurities. The purified sample was then ground to a fine powder (95% minus 325 mesh) in an automatic mortar. One and one half grams of the powdered material was pressed into a bakelite backed pellet at 1400 kg/cm^2, using a hydraulic press. The resulting pellet is 31 mm in diameter by 5 mm thick; actual sample thickness is 1 mm.

Strontium standards

Significant errors may be introduced, in x-ray fluorescence analysis, when samples and standards have substantially different matrices. It was therefore necessary to prepare strontium standards with a barite matrix. According to Hanor (1966) and Heinrich and Vian (1966) some reagent grade barium sulfate contains substantial amounts of strontium. The following procedure,

modified from Hanor (1966) and Gordon et al. (1954),
produced barium sulfate which contained no detectable
strontium when analyzed by x-ray fluorescence spectrometry
(strontium detection limit $\simeq$ 30 ppm).

One hundred grams reagent grade barium chloride was
dissolved in 2 liters distilled water. Twenty milliliters
of concentrated reagent grade hydrochloric acid was added
to prevent precipitation of barium hydroxide or barium
carbonate.

Two and one half milliliters concentrated reagent
grade sulfuric acid was diluted with 50 ml distilled water.

The barium chloride solution was heated to near
boiling, and the diluted sulfuric acid was added slowly
over a period of approximately one minute with constant
vigorous stirring, precipitating barium sulfate.

After a one week digestion period, the solution was
decanted, and the precipitate was thoroughly washed with
distilled water and filtered. The standard barium sulfate
was then dried in a laboratory oven for 24 hours at 100°C.

In preparing the Sr standards, all weighings were done
to 0.1 mg on a Mettler balance. The standards prepared
covered the range from 0.0 to 3.0 mole percent $SrSO_4$.
Standard #S-1 (3.02 m% $SrSO_4$) was prepared by adding a
measured quantity of reagent grade strontium carbonate to a
10.0000 g portion of the standard barium sulfate. In order
to calculate mole percent strontium sulfate the weight of

strontium carbonate was converted to an equivalent weight of strontium sulfate. Strontium carbonate was used because reagent grade strontium sulfate was not available and, according to Hanor (1966), significant quantities of barium may co-precipitate during the synthesis of strontium sulfate from a chloride solution. Standards #S-2 (1.82 m% $SrSO_4$), #S-3 (1.02 m% $SrSO_4$), and #S-4 (0.61 m% $SrSO_4$) were prepared by diluting measured quantities of standard #S-1 with known amounts of the standard barium sulfate. Standard #S-5 (0.12 m% $SrSO_4$) was prepared by diluting a measured quantity of standard #S-3 with a known amount of the standard barium sulfate. Each standard mixture was homogenized in an agate mortar and pelletized for x-ray flouresence spectrometry as described in the previous section.

Analytical Methods

A Siemens x-ray fluorescence analyzer equipped with a gold tube operated at 40 kV and 30 mA, and a scintillation detector operated at 1.0 kV was used for the analyses. Sr K_α radiation (λ = 0.876Å) was dispersed with a LiF crystal (d_{200} = 2.014Å), and counts were accumulated for one minute periods for each sample/standard. Background counts were subtracted, and the net count ratio of sample to standard #S-4 was compared with a standard calibration curve.

The calibration standards were used to construct a calibration curve showing net accumulated count (one minute time) versus mole percent $SrSO_4$ (Figure 28). A working calibration curve was constructed by plotting the ratio of net count for each standard to net count for standard #S-4 (Figure 29). The standard curves shown in Figures 28 and 29 show little deviation from linearity, and intersect at (0,0). The relative probable counting error in these analyses was determined to range from 0.2% to 4.0% at the 1σ confidence level using the equation modified from Stanley (1961):

$$RPE(\%) = \frac{68}{N_p - N_b} (N_p + N_b)^{\frac{1}{2}}$$

where: N_p = accumulated count at peak
N_b = accumulated count at background

Because the calibration standards were not compared with primary external standards the accuracy is difficult to assess. However, the calibration curves shown in Figures 28 and 29 are linear, and the results compare favorably with other analyses cited in the literature (see Figures 30 and 31). The accuracy of the balance used to prepare the standards is probably the most important factor when considering the accuracy of the analyses reported here.

The detection limit for x-ray fluorescence analysis is
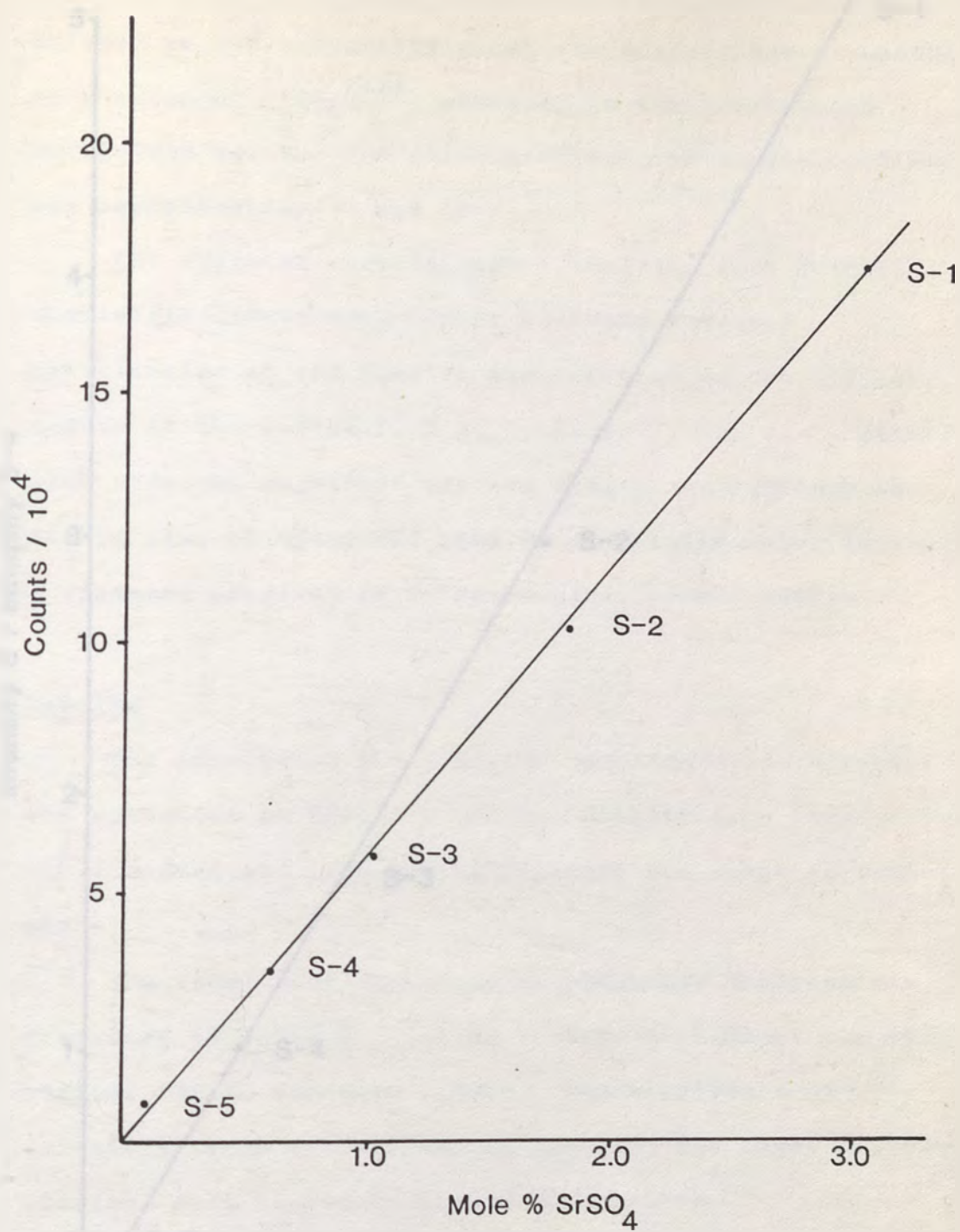
Figure 28   Calibration curve showing net counts (one
minute time) of Sr Kα radiation versus mole
percent strontium sulfate.
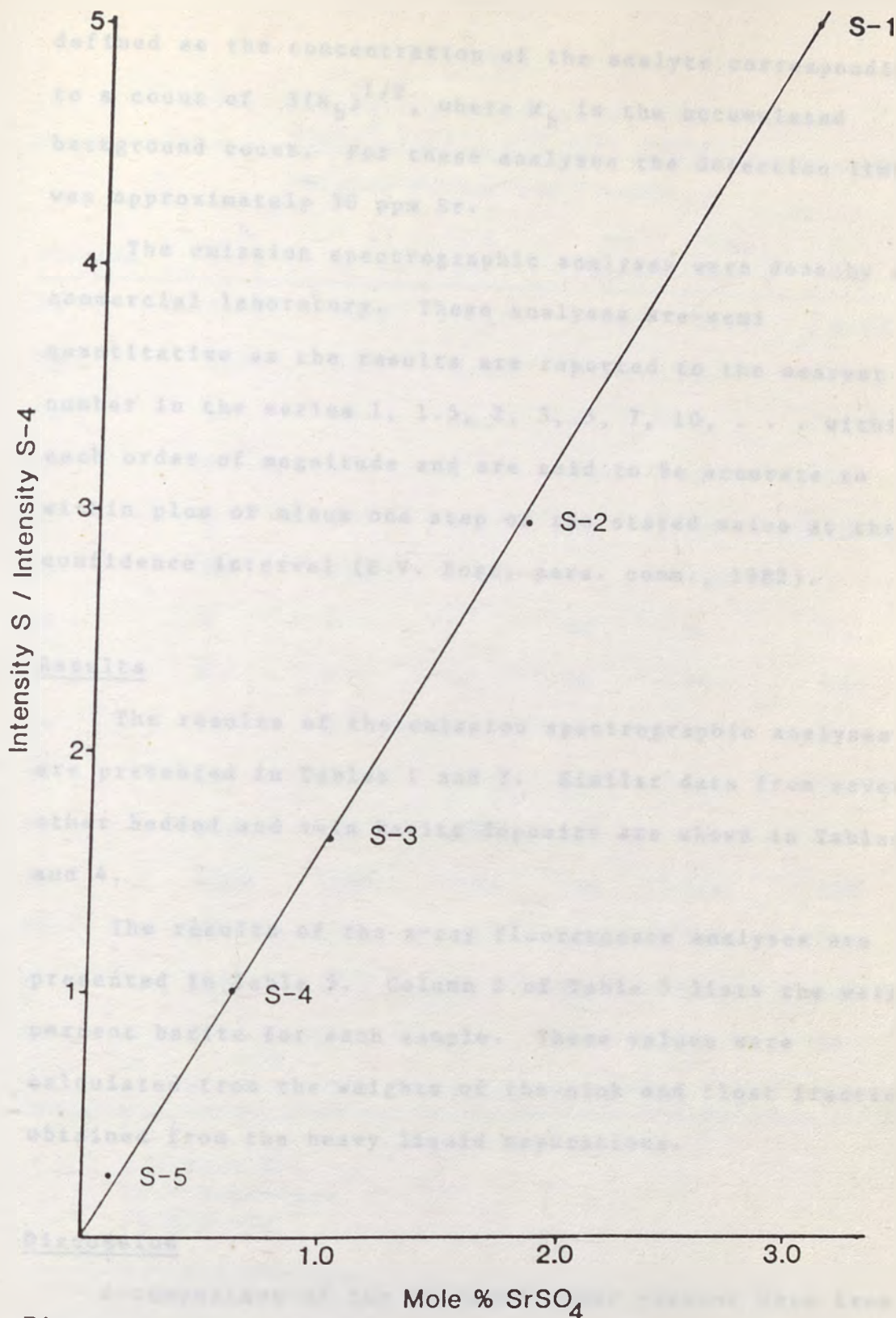
Figure 29   Working calibration curve. All standards
normalized to standard #S-4.

defined as the concentration of the analyte corresponding to a count of $3(N_b)^{1/2}$, where N_b is the accumulated background count. For these analyses the detection limit was approximately 30 ppm Sr.

The emission spectrographic analyses were done by a commercial laboratory. These analyses are semi quantitative as the results are reported to the nearest number in the series 1, 1.5, 2, 3, 5, 7, 10, . . . within each order of magnitude and are said to be accurate to within plus or minus one step of the stated value at the 1σ confidence interval (E.V. Post, pers. comm., 1982).

Results

The results of the emission spectrographic analyses are presented in Tables 1 and 2. Similar data from several other bedded and vein barite deposits are shown in Tables 3 and 4.

The results of the x-ray fluorescence analyses are presented in Table 5. Column 2 of Table 5 lists the weight percent barite for each sample. These values were calculated from the weights of the sink and float fractions obtained from the heavy liquid separations.

Discussion

A comparison of the averaged minor element data from barite at the Almanor, Glidden, and various Nevada bedded

Table 1

Emission spectrographic analyses of Almanor
bedded barite and host rocks.

Sample number and lithology

Element	B A1-2	B A1-10	B A1-9	SS 723-1	Sh 723-4	Det. Lim.
Ca	0.02	0.05	0.15	0.02	0.10	0.02
Mg	0.05	0.02	0.05	0.10	0.07	0.02
Ag	50	20	20	N	N	0.5
Ba	G	G	G	5000	G	10
Cr	N	N	N	N	20	20
Cu	70	100	150	2	100	2
La	N	N	N	20	N	20
Mn	N	N	10	30	20	10
Mo	70	3	10	N	N	3
Ni	10	N	5	5	5	5
Pb	500	200	1000	N	100	10
Sr	2000	2000	7000	100	100	100
Ti	200	10	200	1000	2000	10
V	150	10	150	20	200	10
Zr	N	N	N	200	50	10
Zn	N	1000	1500	N	N	200

B = Barite
SS = Sandstone
Sh = Shale

G = >10,000 ppm
N = Below detection limit

All values are ppm except Ca and Mg which are weight
percent

Table 2

Emission spectrographic analyses of Glidden bedded barite and host rocks.

Sample number and lithology

Element	B Gu-3	B Gl-4	B Gl-3	Sh 720-3	Ls 622-1
Ca	0.15	0.02	0.05	0.07	G
Mg	0.03	0.02	0.05	0.7	0.5
Ag	1	N	N	N	N
Ba	G	G	G	5000	7000
Cr	N	N	N	70	N
Cu	20	N	3	20	2
La	20	20	20	N	N
Mn	100	10	50	150	70
Mo	2	5	10	N	N
Ni	50	N	N	20	N
Pb	10	N	N	10	10
Sr	1000	1500	700	100	200
Ti	700	20	100	2000	100
V	700	100	200	300	10
Zr	20	N	N	100	N
Zn	N	N	N	N	N

B = Barite
Sh = Shale
Ls = Limestone

G = >10,000 ppm
N = Below detection limit (see Table 1)

All values are ppm except Ca and Mg which are weight percent

Table 3

Emission spectrographic analyses of bedded
barite from Nevada

	Deposit or Prospect			
Element	Redhouse	Rossi	Marthalena	Bluerock
Ca	0.03	0.03	0.07	0.15
Mg	0.07	0.03	0.02	0.02
Ag	N	N	N	1
Ba	G	G	G	G
Cr	N	10	10	50
Cu	7	15	20	70
La	20	N	70	70
Mn	10	50	20	30
Mo	2	5	N	N
Ni	5	5	N	30
Pb	10	N	N	10
Sr	2000	1000	2000	3000
Ti	500	150	700	1000
V	200	20	70	300
Zr	20	N	50	100
Zn	N	N	N	N

G = >10,000 ppm
N = Below detection limit (see Table 1)

All values are ppm except Ca and Mg which are weight
percent.

Source: unpublished company report, 1982.

Table 4

Minor element data vein barite

Deposit or Prospect

Element	Trinity	Lunchmeat	Hansen	Mextex
Ca	7	0.7	5	0.01
Mg	2	2	0.05	N
Ag	2	7	N	–
Ba	G	G	G	G
Cr	150	50	10	N
Cu	10	200	15	10
La	N	50	20	–
Mn	1000	500	1000	N
Mo	2	N	N	N
Ni	15	20	N	N
Pb	N	50	100	100
Sr	1000	5000	G	G
Ti	200	1000	500	N
V	30	100	30	N
Zr	N	50	N	N
Zn	N	N	N	N

G = >10,000 ppm
– = No analysis
N = Below detection limit

All values are ppm except Ca and Mg which are weight percent

Trinity, Lunchmeat, and Hansen data from unpublished company reports; Mextex from Brobst (1958).

Table 5

Results of X-ray fluorescence analyses

Glidden deposit

Sample #	Wt. % barite	Mole % $SrSO_4$	Comments
Gu-1a	57	0.18	
Gu-1b	84	0.17	
Gu-1c	94	0.19	
Gu-2a	99	0.18	
Gu-2b	94	0.23	
Gu-2c	-	0.21	
Gu-3a	33	0.13	
Gu-3b	72	0.21	
Gu-3c	78	0.25	
Gu-4a	92	0.16	
Gu-4b	67	0.13	
Gu-4c	63	0.12	
Gu-5	33	0.16	
Gu-7	94	0.23	
Gu-8	79	0.24	
Gu-9	84	0.22	
Gm-1	99	0.20	
Gm-2	95	0.17	
Gl-1	94	0.13	
Gl-2	76	0.23	
Gl-3	73	0.08	
Gl-4	98	0.16	
Gl-5	92	0.07	vein barite

Table 5 (continued)

Alamanor deposit

Sample #	Wt. % barite	Mole % $SrSO_4$	Comments
Al-1	99	0.76	
Al-2	97	0.74	
Al-3	99	0.67	
Al-4	99	0.82	
Al-5	99	0.63	
Al-6	99	0.78	
Al-7	99	0.40	
Al-8	99	0.75	
Al-9	99	0.89	
Al-10	99	0.79	

other deposits (see the Appendix and Fig. 28)

BH	98	2.05	volc. massive $S^=$
Baro	97	0.70	bedded
DG	99	0.52	bedded
BK	97	0.20	bedded
WL	82	1.59	vein
LP	88	0.41	bedded
Demo	99	1.29	bedded
ELP	91	0.65	bedded
TC	96	0.26	bedded
AC	92	0.38	bedded

Table 5 (continued)

Sample #	Wt. % barite	Mole % $SrSO_4$	Comments
PM	94	1.63	volc. massive $S^=$
QA	98	0.55	bedded
Stan	98	2.56	vein
Mil	97	0.15	bedded

barite deposits is shown in Table 6.

Comparing the Almanor and Glidden data reveals the following: Ag, Cu, Mo, Pb and Zn are present in higher concentrations at the Almanor deposit. The Ag content of barite from the Almanor deposit was confirmed by the Nevada Mining Analytical Laboratory, University of Nevada, Reno, Nevada. La and Mn are present in higher concentrations at the Glidden deposit. Other minor elements are present in similar concentrations, where detected, at both deposits.

Comparing the Almanor and Glidden deposits with the various Nevada deposits reveals the following: the minor element suite of Nevada bedded barite is similar to those of the subject deposits, and the abundances of each element are comparable.

A comparison of emission spectrographic data between barite and host rocks (Tables 1 and 2) at each of the subject deposits reveals: Ag, Mo, and Zn were detected in the barite from the Almanor deposit but not in the host rocks. Ag (one sample), La and Mo were detected in the barite from the Glidden deposit but not in the host rocks.

Also included in Table 6 are averaged emission spectrographic data from barite from several vein deposits. Comparison of Almanor, Glidden and Nevada bedded barite with vein barite shows that the trace element suite of bedded and vein barite are similar, and the abundances of each element are comparable. The conclusion that bedded

Table 6

Comparison of averaged minor element
data from barite

	Deposit or type of deposit			
Element	Almanor	Glidden	Nevada	Vein
Ca	0.07	0.07	0.07	3
Mg	0.05	0.03	0.05	1
Ag	30	0.5	0.5	3
Ba	G	G	G	G
Cr	N	N	20	70
Cu	100	7	30	50
La	N	20	50	20
Mn	10	50	30	700
Mo	30	5	3	3
Ni	5	15	10	10
Pb	500	10	10	70
Sr	3000	1000	2000	7000
Ti	150	300	500	500
V	100	300	150	30
Zr	N	10	50	10
Zn	700	N	N	N

G =   >10,000 ppm
N = Below detection limit

All values are ppm except Ca and Mg which are weight
percent.

72

barite is not of hydrothermal origin (Brobst, 1975) does

not seem justified based on minor element data. Indeed,

the similarity in minor element data presented in Table 6

seems to suggest that bedded barite and vein barite could

have a common hydrothermal origin. The presence, in barite

but not in host rocks, of certain minor elements often

associated with hydrothermal ores (Ag, Mo, and Zn at the

Almanor deposit, and Ag and Mo at the Glidden deposit) may

be the result of a hydrothermal introduction of these

elements (and barium) into an otherwise chemically "normal"

sedimentary environment. A comparison of emission

spectrographic data from the various host rocks at the

subject deposits with the average abundance of minor

elements in comparable lithologies is shown in Table 7.

The data of Table 7 show that all host rocks are

considerably enriched in barium over average values for

comparable lithologies. The concentrations of other minor

elements in the various host rocks are not significantly

different from the average values for comparable

lithologies. This suggests that significant quantities of

barium have been introduced into, rather than derived from,

the nearby host rocks.

The strontium content of barite analyzed during this

study ranges from 0.07 to 2.56 mole percent $SrSO_4$. The

strontium content of bedded barite ranges from 0.08 to 1.29

mole percent $SrSO_4$ and that of vein barite and barite

Table 7

Comparison of host rock minor element data with average values for comparable lithologies

| Element | Glidden | | Almanor | | Average | | |
	Sh	Ls	Sh	SS	Sh	Ls	SS
Ca	700	G	1000	200	G	G	G
Mg	7000	5000	700	1000	G	G	7000
Ag	N	N	N	N	0.07	0.0X	0.0X
Ba	5000	7000	G	5000	580	10	X0.0
Cr	70	N	20	N	90	11	35
Cu	20	2	100	2	45	4	X.0
La	N	N	N	20	39	X.0	30
Mn	150	70	20	30	850	1000	X0.0
Mo	N	N	N	N	3	0.4	0.2
Ni	20	N	5	5	68	20	2
Pb	10	10	100	N	20	9	7
Sr	100	200	100	100	300	610	20
Ti	2000	100	2000	1000	4600	400	1500
V	300	10	200	20	130	20	20
Zr	100	N	50	200	160	19	220
Zn	N	N	N	N	95	20	16

G = >10,000 ppm
N = Below detection limit

All values are ppm

Data for average lithologies from Rosler and Lange (1972).

associated with volcanogenic massive sulfides ranges from
0.07 to 2.56 mole percent $SrSO_4$. The lower value reported
for vein barite is from re-mobilized bedded barite at the
Glidden deposit (Sample # Gl-5, Table 5). Excluding this
sample the range for vein barite is 1.59 to 2.56 mole
percent $SrSO_4$. Comparisons of the results obtained during
this study with the results of previous studies are shown
in Figures 30 and 31. The strontium content of each of the
subject deposits appears to have a fairly restricted range
when compared with bedded barite in general (Figure 30).
These narrow ranges may be the result of limited variations
in the physico-chemical environment during barite
mineralization.

Figure 32 shows the cyclic nature of stratigraphic
variations in the strontium content of hand specimen scale
barite samples collected at the Glidden deposit. Samples
Gu-1, Gu-2, Gu-3 and Gu-4 were each cut parallel to bedding
into three 3 cm thick subsamples labeled a, b, and c.
Within each sample, subsample "a" represents the oldest
material, and subsample "c" represents the youngest
material. Samples Gu-7, Gu-8, and Gu-9 are individual,
successive barite laminae, each approximately 3 mm thick,
that were found in place, partly delaminated. In this
sequence, Gu-7 is the oldest material, and Gu-9 is the
youngest material. The cyclic compositional variations
shown in Figure 32 suggest cyclic fluctuations in the
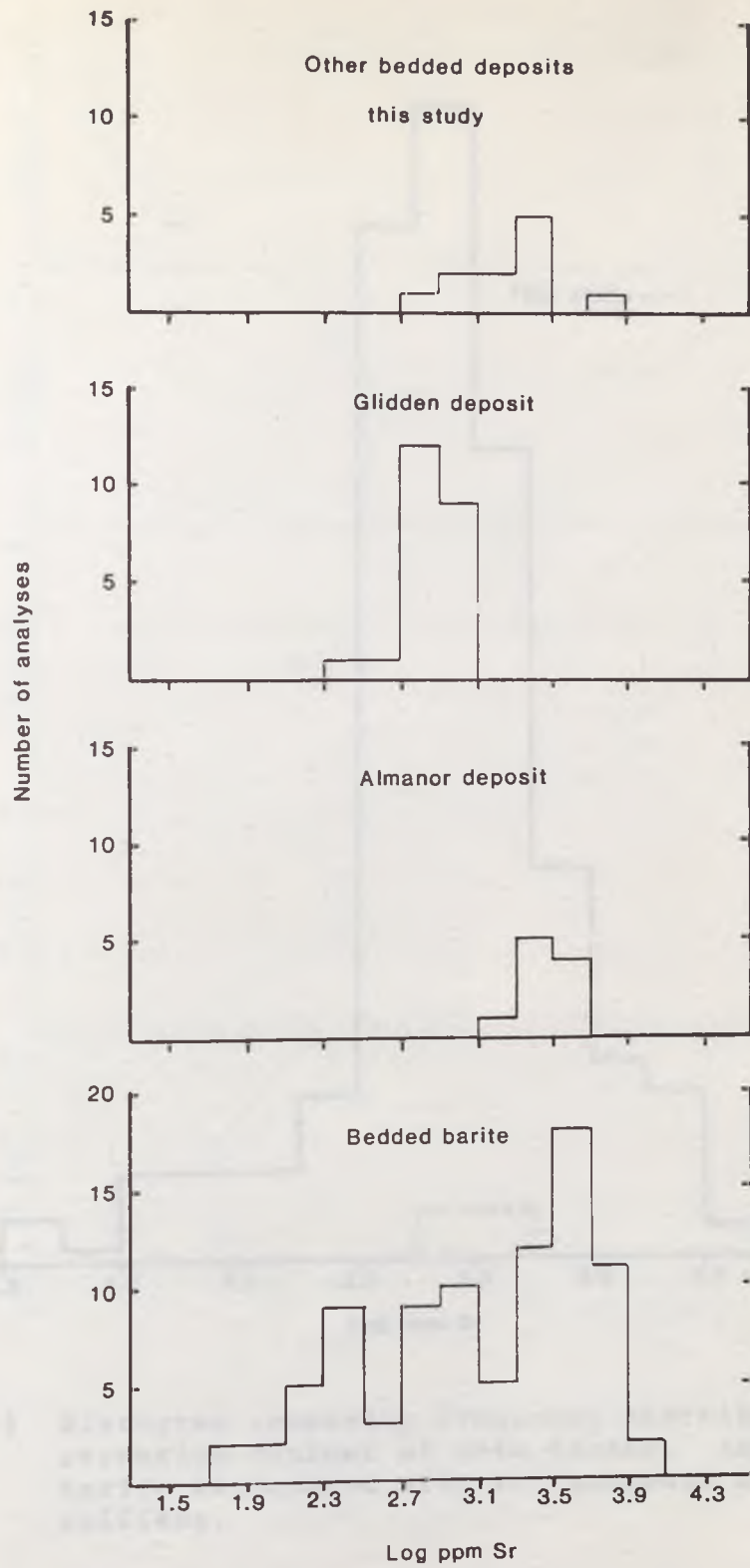
Figure 30   Histograms comparing frequency distributions
             of strontium content of bedded barite.
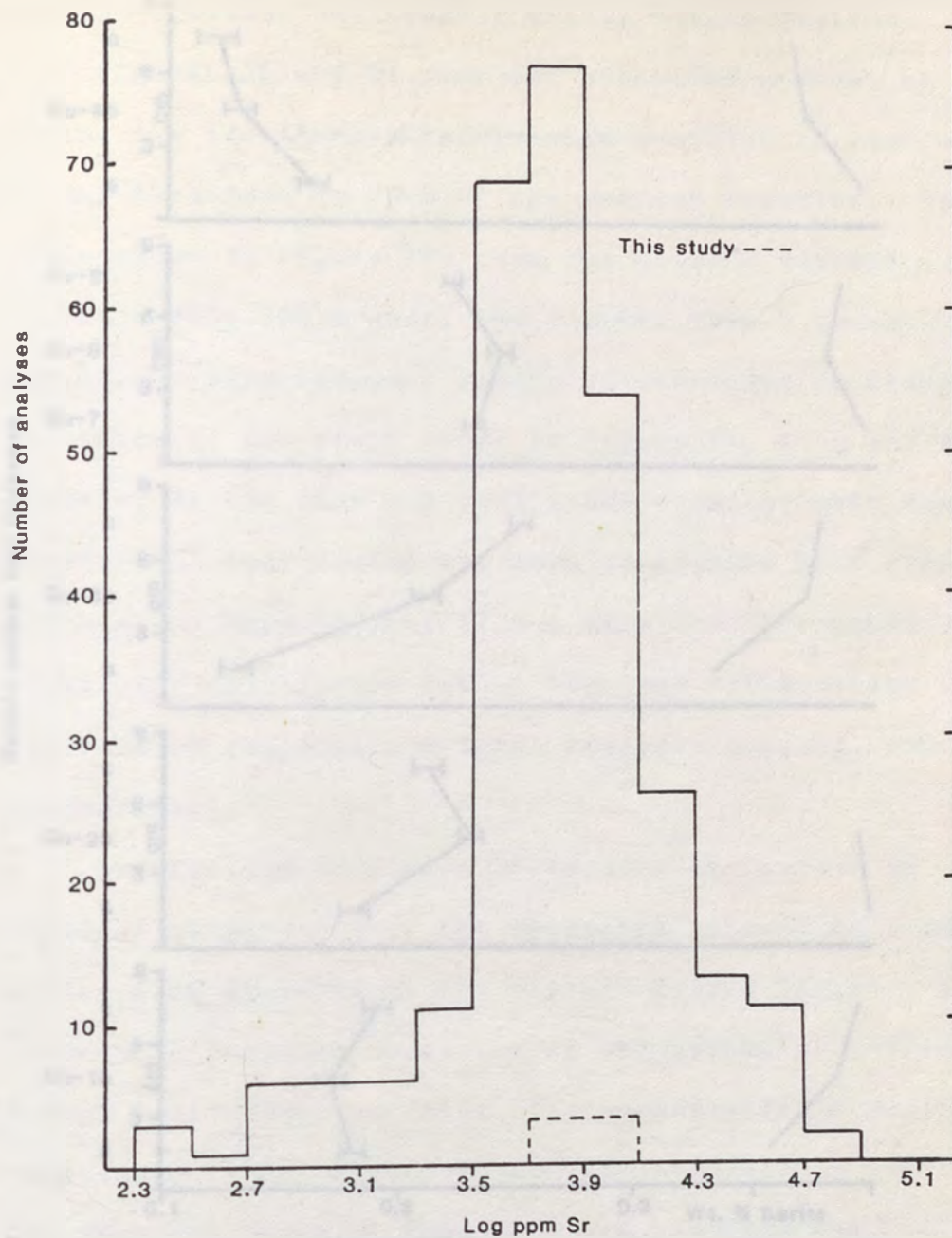
Figure 31   Histogram comparing frequency distributions of strontium content of vein barite.   Includes barite associated with volcanogenic massive sulfides.
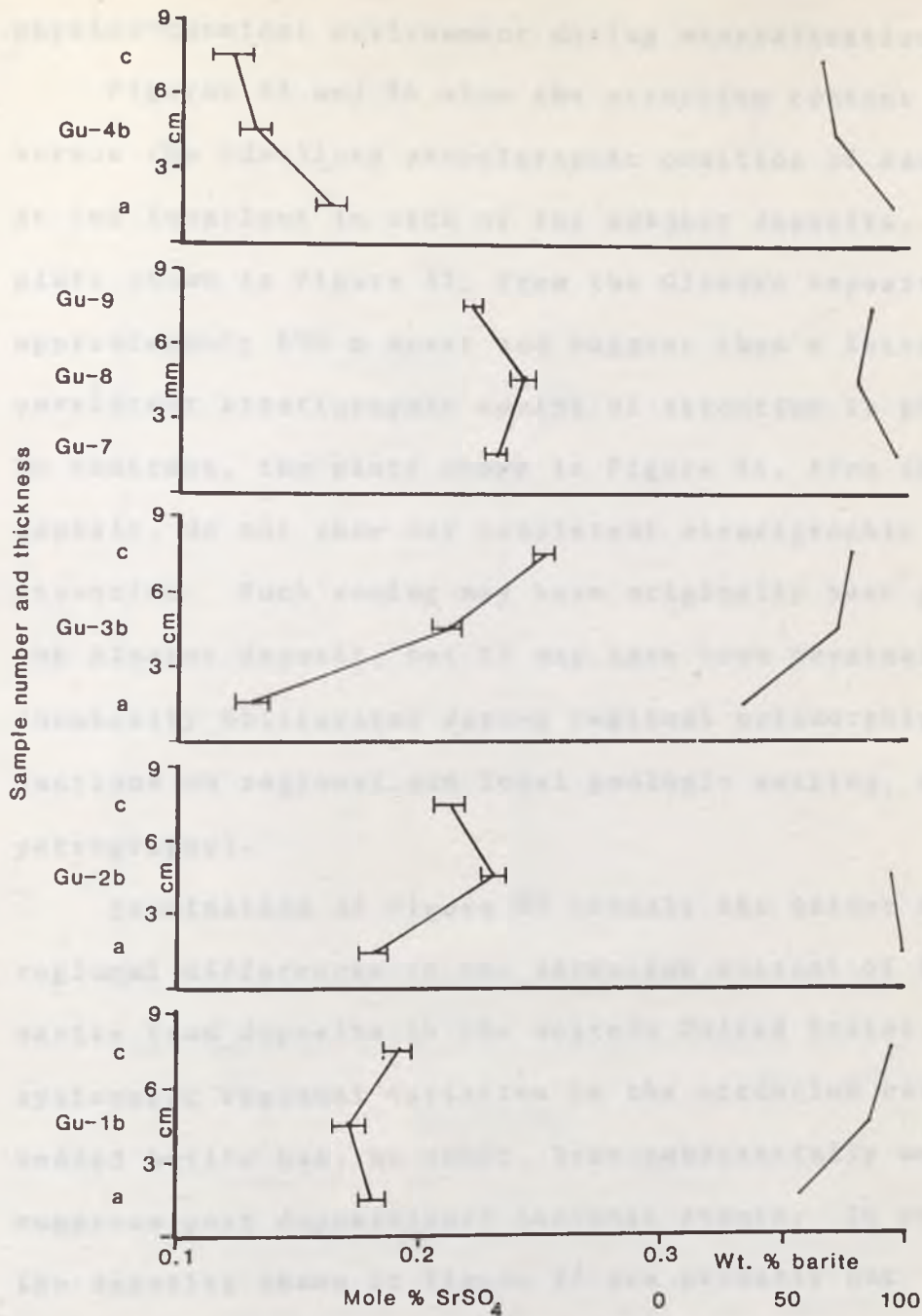
Figure 32 Small scale stratigraphic variations in
strontium content and ore grade of barite at
the Glidden deposit. Width of bars shows
probable counting error.

physico-chemical environment during mineralization.

Figures 33 and 34 show the strontium content of barite versus the idealized stratigraphic position of each sample at two locations in each of the subject deposits. The plots shown in Figure 33, from the Glidden deposit, are approximately 800 m apart and suggest that a laterally persistent stratigraphic zoning of strontium is present. In contrast, the plots shown in Figure 34, from the Almanor deposit, do not show any consistent stratigraphic zoning of strontium. Such zoning may have originally been present at the Almanor deposit, but it may have been physically and/or chemically obliterated during regional metamorphism (see sections on regional and local geologic setting, and petrography).

Examination of Figure 27 reveals the extent of regional differences in the strontium content of bedded barite from deposits in the western United States. Any systematic regional variation in the strontium content of bedded barite has, no doubt, been substantially modified by numerous post depositional tectonic events. In addition, the deposits shown in Figure 27 are probably not contemporaneous. However, it may be significant that the general magnitude of strontium concentrations in bedded barite from California deposits are similar to those of Nevada bedded barite.

Gordon et al. (1954), Cohen and Gordon (1961), Hanor
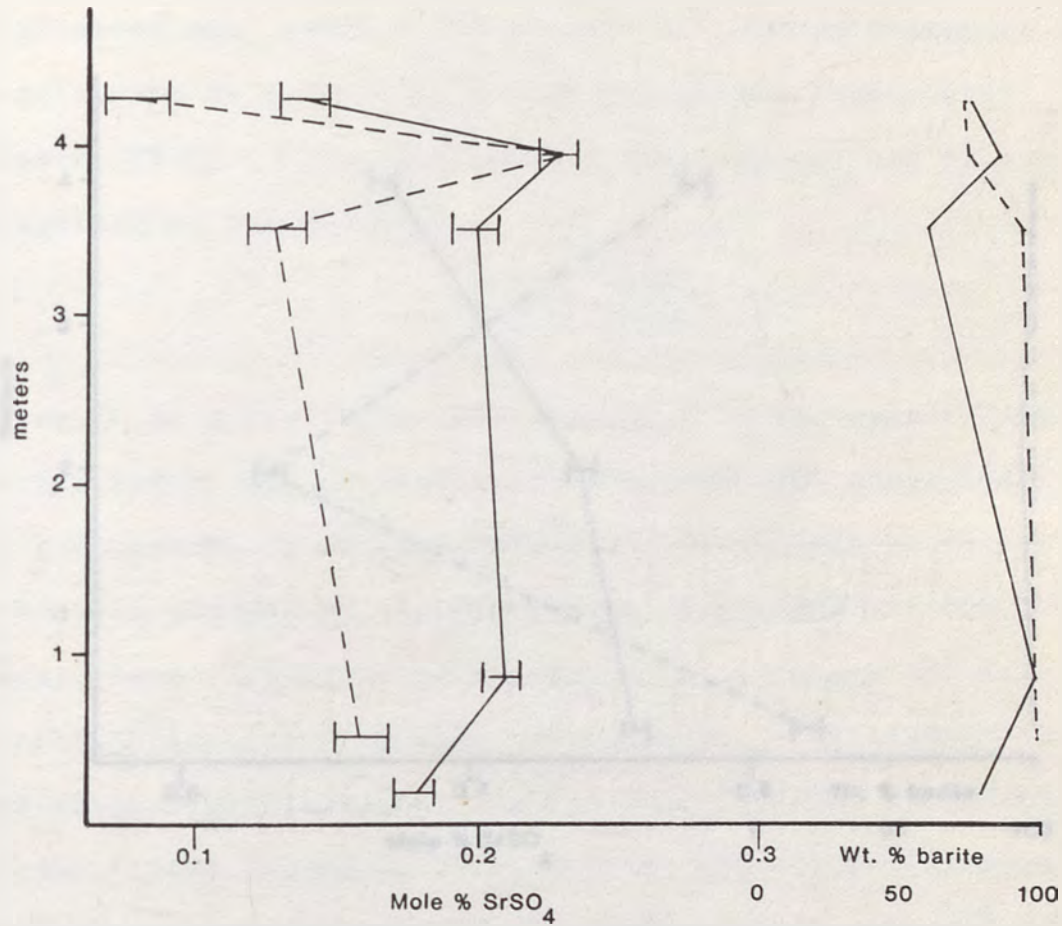
Figure 33   Stratigraphic variation in strontium content and ore grade of barite at the Glidden deposit. Solid line: location 3 Figures 11 and 14, dashed line: location 1 Figures 11 and 14.   Width of bars shows probable counting error.
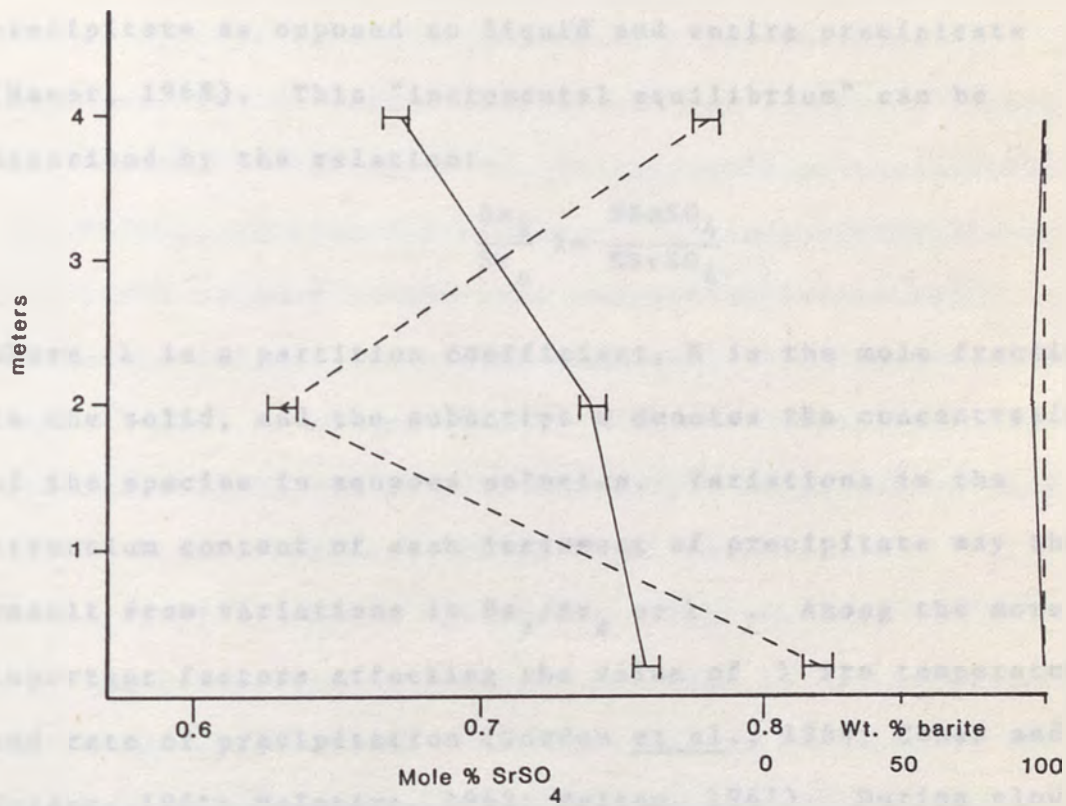
Figure 34   Stratigraphic variation in strontium sulfate content and
            ore grade, Almanor deposit. Solid line: location 1
            Figures 8 and 10; dashed line: location 2 Figures 8 and
            10. Width of bars shows probable counting error.

(1966, 1968, 1969), and Church (1970) have investigated the partitioning of barium and strontium between $(Ba,Sr)SO_4$ and a coexisting aqueous phase. Because $(Ba,Sr)SO_4$ is generally unreactive, equilibrium partitioning is maintained only between liquid and last formed increment of precipitate as opposed to liquid and entire precipitate (Hanor, 1968). This "incremental equilibrium" can be described by the relation:

$$\frac{Ba_s}{Sr_s}\,\lambda = \frac{NBaSO_4}{NSrSO_4}$$

where λ is a partition coefficient, N is the mole fraction in the solid, and the subscript s denotes the concentration of the species in aqueous solution. Variations in the strontium content of each increment of precipitate may then result from variations in Ba_s/Sr_s or λ . Among the more important factors affecting the value of λ are temperature and rate of precipitation (Gordon et al., 1954; Cohen and Gordon, 1961; McIntire, 1963; Walton, 1967). During slow isothermal precipitation of $(Ba,Sr)SO_4$ from a solution with a given starting barium to strontium ratio and in which the sulfate is slowly generated from some other sulfur species (e.g., $H_2S + 2O_2 \rightleftharpoons 2H^+ + SO_4^=$) barium is preferentially partitioned into the solid phase (Gordon, et al., 1954). Later formed increments of barite would therefore contain increasing amounts of strontium due to a decreasing barium to strontium ratio in the aqueous phase. An increased

temperature during the precipitation of any particular increment tends to decrease λ and therefore increase the strontium content of that increment; a decrease in temperature has the opposite effect (Cohen and Gordon, 1961; Church, 1970). An increased rate of precipitation of any particular increment decreases λ and therefore increases the strontium content of that increment (Cohen and Gordon, 1961). However, during rapid precipitation of $(Ba,Sr)SO_4$, as with the mixing of two compositionally different aqueous phases (one containing barium and strontium and one containing sulfate), this "incremental equilibrium" is not established and the composition of the precipitate depends only on the barium to strontium ratio in the aqueous phase, regardless of temperature (i.e., $\lambda \to 1$) (Cohen and Gordon, 1961; Walton, 1977).

From independent geologic evidence it may be possible to decide which of the above factors (or combination of factors) were responsible for the observed variations in strontium content within a particular barite deposit, or between similar barite occurrences.

The high content of interstitial and included material in barite from each of the subject deposits (a portion of which is probably unoxidized organic debris - see Miller et al., 1977), the presence of a fetid odor resembling H_2S in the barite, and the restricted areal extent and lenticular nature of the deposits suggests that barite deposition was

rapid and occurred in small oxygen deficient submarine basins. The massive nature of the lower barite bed at the Glidden deposit also suggests that barite deposition was rapid. Assuming that normal detrital sedimentation was not interrupted during barite deposition, a substantial thickness of fairly pure barite indicates a much higher rate of accumulation of barite over detrital sediments. Because barite is deposited by fluids of high oxidation potential, where sulfur is present as sulfate (Puchelt, 1972), precipitation probably occurred at or above the interface between the oxygen deficient waters in the basin and the overlying sulfate rich seawater. The generally fine grain size of barite from the subject deposits (Figures 17 and 24), suggests rapid precipitation. If so, the compositional variations shown in Figures 32 and 33 are probably the result of variable barium to strontium ratios in the mineralizing fluids during barite precipitation.

Isotopic data agree that the strontium and sulfate in bedded barite from widely separated deposits are derived from seawater (Mitchell, 1977; Rye et al., 1978; Tafuri, 1973; Karunakaran, 1967; Hulen, 1967). Some authors have suggested that the barium in these deposits was also derived from seawater through the dissolution of barium-containing carbonate skeletons (Shawe et al., 1969; Hulen, 1967). Although barite is found as discrete particles in seawater and deep sea sediment cores (Church, 1979; Hanor,

1972), the accumulation rate of these particles is much too slow to account for the barite beds at the subject deposits. This rate of barite accumulation varies from 0.3 µg Ba/cm^2/yr to 3.5 µg Ba/cm^2/yr (Hanor, 1972; Dehairs et al., 1980). At the higher rate a 1 m thick layer of pure barite would accumulate in 70 million years, and at lower rate 800 million years. It is, therefore, logically necessary to seek an alternative source for the barium. The regional geologic settings of both deposits indicates that they originated within or near a Klamath-Sierran volcanic arc complex. It is possible that hydrothermal fluids associated with this arc complex were a source of barium.

ORIGIN OF THE BARITE DEPOSITS, A GENETIC MODEL

Several different models have been proposed to explain
the origin of bedded barite in the Western United States.
This diversity suggests that no single model is completely
satisfactory. Many of the uncertainties associated with
these genetic schemes are, no doubt, due to the tectonic
shuffling of the host "Antler Belt" sediments and to the
consequent inability to define a specific geologic setting
in which the barite was deposited. In contrast, the host
rocks at the subject deposits, although metamorphosed and
possibly allochthonous, are not tectonically interleaved
and thus provide a more reliable geologic basis for genetic
interpretation.

Hydrothermal convection of seawater, driven by cooling
intrusive bodies within the Paleozoic Klamath-Sierran
volcanic arc, may leach barium from the porous sediments
and volcanic rocks of the arc complex. Reduction of
seawater sulfate through heating and chemical reactions
with the volcanic rocks would greatly enhance the barium
leaching and transporting capability of such a convecting
fluid. Hydrothermal waters venting at the 21° North site
of the East Pacific Rise, and similar thermal waters from
the Galapagos Rift are considerably enriched in barium and
depleted in sulfate, but have similar concentrations of
strontium when compared with seawater (Corliss et al.,

1979; Edmond et al., 1982). Magmatic water derived from the cooling intrusives may also supply dissolved barium. Faults and fractures provide likely conduits to the sea floor for these heated, barium rich fluids. As these heated fluids encounter sulfate rich seawater within the conduits and/or sediments, barite is precipitated. Depletion of the seawater sulfate in these regions would allow the dissolved barium to be exhaled into the overlying seawater where an essentially infinite supply of sulfate is available. Upon mixing with seawater, barite would rapidly precipitate and be deposited in or near the vent area. Continued exhalation of such a fluid would produce a strataform bed of barite underlain by stockwork and/or disseminated barite mineralizaton. Barite deposited from sea floor hot springs has been observed in the South San Clemente Basin, southwest of San Diego (Lonsdale, 1979), in the Lau Basin, northeast of Australia (Bertine and Keene, 1975), and on the Baja Peninsula (L.T. Larson, pers. comm., 1983). Frequently associated with such submarine hot springs are abundant benthic fauna whose feeding habits attract them to the thermal vent areas (Lonsdale, 1979; Corliss et al., 1979). Presumably, similar hot spring systems could be established within volcanic island arc settings (Snyder, 1978). In fact, Urabe and Sato (1978) proposed that the strataform barite bodies capping the Kuroko massive sulfide deposits of Japan formed from the

mixing of exhalative barium rich solutions and seawater in an island arc setting. However, stockwork or disseminated barite mineralization was not observed to underlie the subject deposits and baritized fossils were not found. This suggests that barite deposition occurred some distance from any exhalative vent area. In addition, the fetid odor of H_2S, invariably present when barite from the subject deposits is broken or crushed, suggests that barite deposition occurred within a euxinic basin. According to Sato (1972, cited in Carne, 1979) certain exhalative fluids may be considerably denser than seawater, and could thus be expected to flow down slope away from the exhalative vent, and eventually pool in a closed basin. Turner and Gustafson (1978) show that these dense fluids could flow for tens or even hundreds of kilometers before encountering a closed basin. Furthermore, Sakai and Matsubaya (1974) suggest that such fluids may contain substantial quantities of barium. Periodic mixing of the pooled barium rich fluid and the overlying sulfate rich seawater would produce laminae of fine grained barite intercalated within any sediments that are accumulating in such a basin. This mixing may be the result of storm generated turbulence within the overlying seawater, seismic disturbances, or periodic input of fresh ore bearing solution that would tend to lift previously ponded ore fluid (Turner and Gustafson, 1978) and allow mixing with seawater.

Alternatively, fresh solution input may be fairly continuous, and precipitation of barite at the interface between the ponded ore solution and seawater would produce a steady "snowfall" of fine grained barite that would sink and accumulate on the floor of the basin. Thus the interlayering of barite and sediment would be the result of continuous barite deposition and varying rates of detrital sedimentation. However, it seems likely that both detrital sedimentation and barite deposition rates were variable. Subsequent diagenetic recrystallization of this fine grained barite would tend to increase grain size, possibly enclosing organic and inorganic sedimentary material dispersed within the volumetrically greater amount of barite.

Assuming that these exhalative solutions were, for the most part, derived from seawater, and that the strontium content of such solutions are essentially the same as seawater (e.g. Corliss et al., 1979; Edmond et al., 1982), then variations in the strontium content of the rapidly precipitated barite would be the result of variable concentrations of barium in the mineralizing fluid. This mineralizing fluid is composed of a mixture of exhalative hydrothermal fluid and seawater. Although the variation in exhalative fluid composition from different vent areas (e.g. Corliss et al., 1979) may explain the variation in strontium content of widely separated bedded barite

deposits (Figure 27), the narrow range of strontium concentrations within a single deposit (Figure 30) suggests that the fluid composition from a single vent area is fairly constant. The cyclic compositional variations shown in Figure 32 may therefore be the result of periodic input of a fresh batch of exhalative fluid. As one batch of exhalative fluid is gradually mixed with seawater barite precipitation occurs. This precipitation would remove barium and strontium from the mineralizing fluid. However, an essentially infinite supply of strontium in seawater would tend to "buffer" the concentration of this element, and the barium to strontium ratio of the mineralizing fluid would drop. Continued gradual mixing with seawater would therefore produce barite containing increasing amounts of strontium. Input of a fresh batch of exhalative fluid would start the cycle again. Alternatively, the concentration of barium and strontium in a particular batch of mineralizing fluid may become so dilute that the precipitation rate of barite is significantly reduced. Under such conditions the barium is preferentially partitioned over strontium into the solid phase (barite). Thus slowing the rate of precipitation may cause a decrease in the strontium content of the barite.

This variable mixing model can also be used to explain the variation in strontium content of barite from deposit to deposit, assuming a common or compositionally comparable

source (s). As an exhalative fluid is flowing downslope

away from the vent, some mixing with seawater is likely to

occur. Precipitation of barite during this limited mixing

would tend to lower the barium to strontium ratio of the

mixture. Barite precipitated farther and farther from the

vent area would contain greater and greater amounts of

strontium. However, it seems likely that there is a limit

to this increasing strontium content of barite with

distance from the vent. Continued precipitation of barite

from the mineralizing fluid while flowing away from the

vent would eventually lower the barium concentration of the

fluid to a point where barite no longer precipitates, or

the amount available for precipitation after pooling is

quantitatively insignificant. The essential elements of this

model are presented in Figure 35.
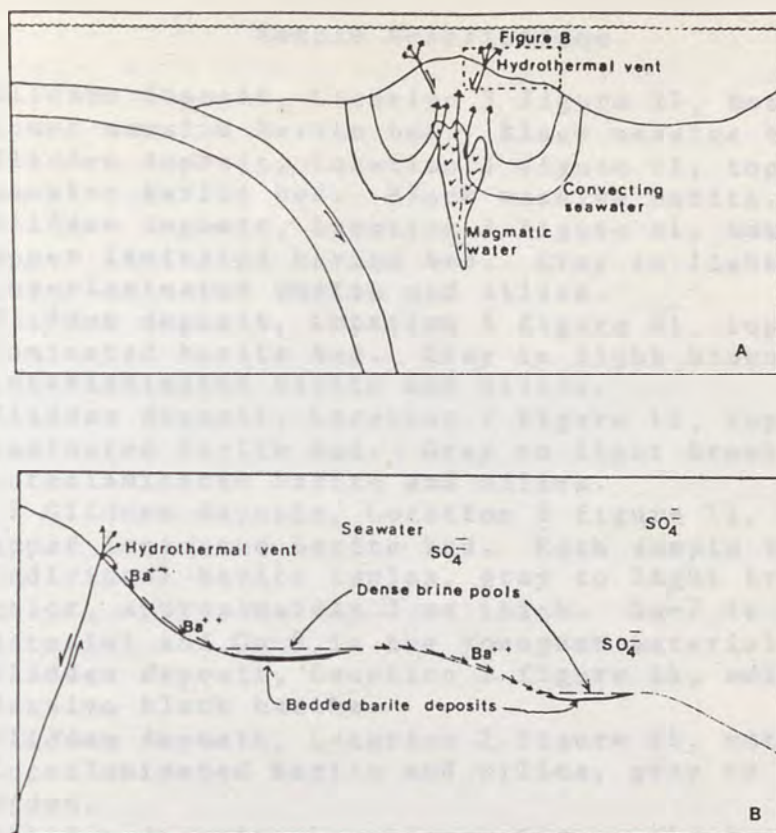
Figure 35   Proposed model for bedded barite mineralization. Part A:
Convecting seawater leaches barium from the rocks of a
volcanic arc complex. Magmatic water may also supply
dissolved barium. The heated barium-rich fluids are
channeled through faults and fractures, and vented into the
overlying seawater. Part B (Dashed outlined area around
hydrothermal vent of part A is shown enlarged as part B):
The dense barium-rich hydrothermal fluid flows downslope,
away from the exhalative vent, and eventually pools in a
closed depression. At the interface between the dense
brine pools and the sulfate-rich seawater fine grained
barite is precipitated, and sinks to accumulate on the
floor of the closed basin.

APPENDIX

Sample Descriptions

Gu-1 Glidden deposit, Location 3 figure 11, bottom of
      lower massive barite bed. Black massive barite.
Gu-2 Glidden deposit, Location 3 figure 11, top of lower
      massive barite bed. Black massive barite.
Gu-3 Glidden deposit, Location 3 figure 11, bottom of
      upper laminated barite bed. Gray to light brown
      interlaminated barite and silica.
Gu-4 Glidden deposit, Location 3 figure 11, top of upper
      laminated barite bed. Gray to light brown
      interlaminated barite and silica.
Gu-5 Glidden deposit, Location 3 figure 11, top of upper
      laminated barite bed. Gray to light brown
      interlaminated barite and silica.
Gu-7,8,9 Glidden deposit, Location 3 figure 11, middle of
      upper laminated barite bed. Each sample is an
      individual barite lamina, gray to light brown in
      color, approximately 3 mm thick. Gu-7 is the oldest
      material and Gu-9 is the youngest material.
Gm-1 Glidden deposit, Location 2 figure 11, not in place.
      Massive black barite.
Gm-2 Glidden deposit, Location 2 figure 11, not in place.
      Interlaminated barite and silica, gray to light
      brown.
Gl-1 Glidden deposit, Location 1 figure 11, bottom of
      upper laminated barite bed. Gray to light brown
      interlaminated barite and silica.
Gl-2 Glidden deposit, Location 1 figure 11, middle of
      upper laminated barite bed. Gray to light brown
      interlaminated barite and silica.
Gl-3 Glidden deposit, Location 1 figure 11, top of upper
      laminated barite bed. Gray to light brown
      interlaminated barite and silica.
Gl-4 Glidden deposit, Location 1 figure 11, middle of
      lower massive barite bed. Black massive barite.
Gl-5 Glidden deposit, Location 1 figure 11, iron stained,
      finely crystalline vein barite.
622-1 Glidden deposit, very fine grained blue limestone
      above barite horizon, numerous fossils, Kennett
      Formation.
720-3 Glidden deposit, black shale-slate, weathers gray
      around edges, below barite horizon, Kennett
      Formation.
Al-1 Almanor deposit, Location 1 figure 8, bottom of lower
      barite bed. Black massive barite with barite
      porphyroclasts set in a matrix of fine grained
      barite.
Al-2 Almanor deposit, same location as Al-1, bottom of
      upper barite bed, black laminated to massive barite.
Al-3 Almanor deposit, same location as Al-1, top of upper

barite bed, black to gray massive to laminated barite.

A1-4   Almanor deposit, Location 2 figure 8, bottom of lower barite bed. Black massive barite with numerous porphyroclasts of barite.

A1-5   Almanor deposit, same location as A1-4, bottom of upper barite bed, black massive barite with numerous porphyroclasts of barite.

A1-6   Almanor deposit, same location as A1-4, top of upper barite bed, black massive barite with numerous porphyroclasts of barite.

A1-7   Almanor deposit, Location 4 figure 8, North end of deposit, black massive barite with numerous barite porphyroclasts. From middle of lower barite bed.

A1-8   Almanor depsit, same location as A1-7, black massive barite, from middle of upper barite bed.

A1-9   Almanor deposit, from Location 3 figure 8, black to gray massive barite.

A1-10 Alamnor deposit, Location 5 figure 8, black to gray massive barite.

723-1 Almanor deposit, fine grained extremely hard quartzite lens above barite horizon.

723-4 Almanor deposit, argillite-shale layer below barite horizon.

BH   Bully Hill mine, East Shasta district. Light yellow massive barite with some sulfides.

Baro From Baro claim group, secs. 10, 15 T22S R34E MDB&M, white sugary textured recrystallized barite associated with Paleozoic (?) sediments in Sierran roof pendant.

DG   Devils Gulch deposit, secs. 17, 20 T4S R20E MDB&M, white recrystallized barite. Associated with "lower" Shoo Fly Complex.

BK   Barite King claim group, Ninemile Canyon deposit, secs. 26, 34, 35 T23S R36E & sec. 2 T24S R36E MDB&M. Light brown iron stained barite associated with Paleozoic (?) sediments in Sierran Roof Pendant.

WL   Waterloo deposit, sec. 16 T10N R1E SBM. Red to brown iron stained vein barite

LP   La Paloma claims, Camp Nelson deposit, sec 33 T20S R31E and Sec. 3 T21S R31E MDB&M. Light gray barite associated with Paleozoic (?) sediments in Sierran roof pendant.

Demo Democrat deposit, sec. 24 T16N R10E MDB&M. Gray to black massive barite with barite porphyroclasts, very similar in appearance to Almanor barite. Associated with "Lower (?)" Shoo Fly Complex.

ELP   El Portal deposit, secs. 18, 19 T3S R20E MDB&M. Light gray, recrystallized barite. Associated with Paleozoic "western facies" sediments.

TC   Taylor Canyon prospect, near Tuscarora, Elko County, Nevada. Brown bedded barite. Associated with Paleozoic "western facies" sediments.

AC Anderson Canyon deposit, near Winnemucca, Humboldt County, Nevada. Brown bedded barite. Associated with the Cambrian Preble Formation (?).

QA Queen Ann deposit, near Carlin, Eureka County, Nevada. Gray to brown bedded barite. Associated with Paleozoic "western facies" sediments.

Mil T.L. Miller claims, Mineral County, Nevada. Gray bedded barite. Associated with Ordovician Palmetto formation (?).

Stan Stansbury Mountains, Utah. Clear to white crystalline vein barite. Associated with Paleozoic carbonates.

PM Peck Mountain prospect, Idaho. Clear to white barite associated with volcanogenic massive sulfides.

REFERENCES

Albers, J.P., and Robertson, J.F., 1961, "Geology and Ore Deposits of the East Shasta Copper-Zinc District Shasta County, California", U.S.G.S. Prof. paper 338

_____, Kistler, R.W., and Kwak, L., 1981, "The Mule Mountain Stock, An Early Middle Devonian Pluton in Northern California", Isochron/West, No. 31

Averill, C.V., 1939, "Barite", California Division of Mines and Geology, Journal of Mines and Geology v. 35, pp. 114-115

Barbieri, M., Masi, U., and Tolomeo, L., 1982, "Strontium Geochemistry in the Epithermal Barite Deposits from the Apuan Alps (Northern Tuscany, Italy)", Chemical Geology, v. 35, pp. 351-356

Bertine, K.K. and Keene, J.B., 1975, "Submarine Barite Opal Rocks of Hydrothermal Origin", Science, v. 188, pp. 150-152

Bogoch, R., and Shirav, M., 1978, "Petrogenesis of a Senonian Barite Deposit, Judean Desert, Israel", Mineral. Deposit., v. 13, pp. 383-390

Bond, G.C., Menzies, M., and Moores, E.M., 1977, Guidebook: Paleozoic-Mesozoic Rocks of the Northern Sierra Nevada, U.C. Davis

_____, and Devay, J.C., 1980, "Pre Upper Devonian Quartz Sandstones in the Shoo Fly Formation, Northern California - Petrology, Provenance, and Implications for Regional Tectonics", Jour. of Geol., v. 88, pp. 285-308

Boucot, A.J., Dunkle, P.H., Potter, A.W., Savage, N.M., and Rohr, D.M., 1974, "Middle Devonian Orogeny in Western North America? A Fish and other Fossils", Jour. of Geol., v. 82, pp. 691-708

Brobst, D.A., 1958, "Barite Resources of the United States", U.S.G.S. Bull. 1072B, pp. 67-130

_____, Pinckney, D.M., and Sainsbury, C.L., 1971, "Geology and Geochemistry of the Sinuk River Barite Deposit, Seward Peninsula, Alaska", U.S.G.S. Prof. paper 750D, pp. D1-D8

_____, 1975, "Barium Minerals" in: J.L. Gillison, ed., Industrial Minerals and Rocks, 3rd ed., AIME, pp. 427-442

Campbell, F.A., 1959, "The Geology of the Torbrit Silver Mine", Econ. Geol., v. 54, pp. 1461-1495

Carne, R.C., 1979, "Geological Setting and Stratiform Mineralization Tom Claims, Yukon Terrtory", open file rept. EGS 1979-4, Dept. Indian and Northern Affairs

Cashman, S.M., 1980, "Devonian Metamorphic Event in the Northeastern Klamath Mountains, California", G.S.A. Bull., Part I, v. 91, pp. 453-459

Church, T.M., 1970, "Marine Barite", Ph.D. Thesis, U.C. San Diego

_____, 1979, "Marine Barite", in: R.G. Burns, ed., Marine Minerals, Miner. Soc. of Amer., Short course notes, pp. 180-207

Churkin, M., and Eberlein, G.D., 1977, "Ancient Borderland Terrains of the North American Cordillera: Correlations and Microplate Tectonics", G.S.A. Bull., v. 88, pp. 769-786

Clark, C.N., 1970, "Trace Elements in Missouri Barite", M.S. Thesis, Univ. of Missouri

Clark, L.D., 1976, "Stratigraphy of the North Half of the Western Sierra Nevada Metamorphic Belt", U.S.G.S. Prof. paper 923

Cohen, A.I., and Gordon, L.G., 1961, "Co-precipitation in some Binary Sulfate Systems", Talanta, v. 7, pp. 195-211

Condie, K.C., and Snansieng, S., 1971, "Petrology and Geochemistry of the Duzel (Ordovician) and Gazelle (Silurian) Formations, Northern California", Jour. of Sed. Pet., v. 41, pp. 741-751

Corliss, J.B., and 10 others, 1979, "Submarine Thermal Springs on the Galapagos Rift", Science, v. 203, pp. 1073-1083

D'Allura, J.A., 1977, "Stratigraphy, Structure, Petrology and Regional Correlations of Metamorphic Upper Paleozoic Volcanic Rocks in parts of Plumas, Sierra, and Nevada Counties, California", Ph.D. thesis, U.C. Davis

_____, Moores, E.M., and Robinson, L., 1977, "Paleozoic Rocks of the Northern Sierra Nevada: Their Structural and Paleogeographic Implications", in: Stewart, J.H., Stevens, C.H., and Fritsche, A.E., eds., Paleozoic Paleogeography of the Western United States, SEPM, Pacific Section, Pacific Coast Paleogeography Symposium 1, pp. 395-408

Davis, G.A., 1969, "Tectonic Correlations, Klamath Mountains and Western Sierra Nevada, California", G.S.A. Bull., v. 80, pp. 1095-1108

Dehairs, F., Chesselet, R., and Jedwab, J., 1980, "Descrete Suspended Particles of Barite and the Barium cycle in the Open Ocean", Earth and Planetary Sci. Letters, v. 49, pp. 528-550

Diller, J.S., 1892, "Geology of the Taylorsville region of California", G.S.A. Bull. v. 3, pp. 370-394

_____, and Schuchert, C., 1894, "Discovery of Devonian Rocks in California", Amer. Jour. of Sci., v. 47, pp. 416-422

_____, 1905, "The Bragdon Formation", Amer. Jour. of Sci., v. 4, pp. 379-387

_____, 1906, "Description of the Redding Quadrangle", U.S.G.S. Geologic Atlas, Redding Folio no. 138

_____, 1908, "Geology of the Taylorsville Region, California", U.S.G.S. Bull. no. 353, 128p

Edmond, J.M., Von Damm, K.L., McDuff, R.E., and Measures, C.I., 1982, "Chemistry of Hot Springs on the East Pacific Rise and Their Effluent Dispersal", Nature, v. 297, pp. 187-191

Fairbanks, H.W., 1894, "Localities of Mesozoic and Paleozoic in Shasta County, California", Amer. Geologist, v. 14, pp. 25-31

Friedman, G.M., and Sanders, J.E., 1978, Principles of Sedimentology, John Wiley

Girty, G.H., 1983, "The Culbertson Lake Allochthon, a newly identified structural unit within the Shoofly Complex: sedimentologic, stratigraphic, and structural evidence for extension of the Antler Orogenic Belt to the Northern Sierra Nevada, California," Ph.D., thesis, Columbia University

Gordon, L.G., Reimer, C.C., and Burtt, B.P., 1954, "Distribution of Strontium within Barium Sulfate Precipitated from Homogeneous Solution", Anal. Chem., v. 26, pp. 842-846

Graton, L.C., 1909, "The Occurrence of Copper in Shasta County, California", U.S.G.S. Bull. 430B, pp. 71-111

Hannah, J.L., 1981, "Stratigrahy, Petrography, Paleomagnetism, and Tectonics of Paleozoic Arc Complexes, Northern Sierra Nevada, California", Ph.D. thesis, U.C. Davis

_____, and Verosub, K.L., 1980, "Tectonic Implications of Remagnetized Upper Paleozoic Strata of the Northern Sierra Nevada", Geology v. 8, pp. 520-524

Hanor, J.S., 1966, "The Origin of Barite", Ph.D. thesis, Harvard Univ.

_____, 1968, "Frequency Distribution of Compositions in the Barite-Celestite Series", Amer. Miner., v. 53, pp. 1215-1222

_____, 1969, "Compositional Zoning in Concretions", G.S.A. Abstracts w/Progs., part 7, pp. 89

_____, 1972, "Rate of Barium Accumulation in the Equitorial Pacific", G.S.A. Abstracts w/Progs. v. 4, p. 526

Heinrich, E.W., and Vian, R.W., 1966, "Carbonatitic Barites", Amer. Miner., v. 52, pp. 1179-1189

Hershey, O.H., 1901, "Metamorphic Formations of Northwestern California", Amer. Geologist, v. 27, pp. 225-245

Hinds, N.E.A., 1932, "Paleozoic Eruptive Rocks of the Southern Klamath Mountains", Calif. Univ. Pub. Geol. Sci., Bull., v. 20, pp. 375-410

Hopson, C.A., and Mattinson, J.M., 1973, "Ordovician and Late Jurassic Ophiolitic Assemblages in the Pacific Northwest", G.S.A. Abstracts w/Progs. v. 5, p. 57

Hulen, P.L., 1967, "Determination of the Source of Barite in the Chamberlain Creek Deposit of Arkansas: Sr Isotopic Evidence", M.S. thesis, Univ. of Kansas

Irwin, W.P., 1960, "Geologic Reconnaissance of the Northern
    Coast Ranges and Klamath Mountains, California, with a
    Summary of Mineral Resources", Calif. Div. Mines
    Bull. 179

_____, 1977, "Review of Paleozoic Rocks of the Klamath
    Mountains", in: Stewart, J.H., Stevens, C.H., and
    Fritsche, A.E., eds., Paleozoic Paleogeography of the
    Western United States, SEPM, Pacific Section, Pacific
    Coast Paleogeography Symposium 1, pp. 441-454

_____, 1981, "Tectonic Accretion of the Klamath Mountains",
    in: Ernst, W.G., ed. The Geotectonic Development of
    California, Rubey volume 1, pp. 29-49, Prentice-Hall

Karunakaran, C., 1976, "Sulfur Isotopic Composition of
    Barite and Pyrites from Mangampeta, Cuddapah District,
    Andhra Pradesh", Jour. Geol. Soc. of India, v. 17, pp.
    181-185

Ketner, K.B., 1965, "Economic Geology", in: Gilluly, J.,
    and Gates, O., Tectonic and Igneous Geology of the
    Northern Shoshone Range Nevada, U.S.G.S. Prof. paper
    465, pp. 129-143

Kinkle, A.R., Hall, W.E., and Albers, J.P., 1956, "Geology
    and Base Metal Deposits of the West Shasta Copper Zinc
    District, Shasta County, California", U.S.G.S. Prof.
    paper 285

Leach, D.L., 1980, "Nature of Mineralizing Fluids in the
    Barite Deposits of Central and Southeast Missouri",
    Econ. Geol., v. 75, pp. 1168-1180

Lindsley-Griffith, N., 1977, "Paleogeographic Implications
    of Ophiolites: the Ordovician Trinity Complex, Klamath
    Mountains, California", in: Stewart, J.H., Stevens,
    C.H., and Fritsche, A.E., eds., Paleozoic
    Paleogeography of the Western United States, SEPM,
    Pacific Section, Pacific Coast Paleogeography
    Symposium 1, pp. 409-420

_____, 1982, "Structure, Stratigraphy, Petrology, and
    Regional Relationships of the Trinity Ophiolite,
    Eastern Klamath Mountains, California", Ph.D. thesis,
    U.C. Davis

Lonsdale, P., 1979, "A Deep-sea Hydrothermal Site on a
    Strike-slip Fault", Nature, v. 281, pp. 531-534

Mariano, A.N., 1980, "A Study of Barite from the Mountain
    Pass Carbonatite", report to Molybdenum Corp. of
    America, Mountain Pass, California

McIntire, W.L., 1963, "Trace Element Partition Coefficients
    - a Review of Theory and Applications to Geology",
    Geochem. et Cosmochim. ACTA, v. 27, pp. 1209-1264

McMath, V.E., 1958, "Geology of the Taylorsville area,
    Plumas County, California", Ph.D. thesis, U.C.L.A.

_____, 1966, "Geology of the Taylorsville area, Northern
    Sierra Nevada, California", Calif., Div. Mines and
    Geol. Bull. 190, pp. 173-183

Miller, R.E., Brobst, D.A., and Beck, P.C., 1977, "The
    Organic Geochemistry of Black Sedimentary Barite:
    Significance and Implications of Trapped Fatty Acids",
    Organic Geochemistry, v. 1, pp. 11-26

Mitchell, W., 1977, "Geology of Some Bedded Barite Deposits
    of North Central Nevada", M.S. thesis, Univ. of
    Nevada, Reno

Moen, W.S., 1964, "Barite in Washington", Wash. Div. Mines
    and Geol. Bull. 51

Moores, E., 1970, "Ultramafic and Orogeny, with Models of
    the U.S. Cordillera and the Tethys", Nature, v. 228,
    pp. 837-842

Morrow, D.W., Krouse, H.R., Ghent, E.D., Taylor, G.C., and
    Dawson, K.R., 1978, "A Hypothesis concerning the
    Origin of Barite in Devonian Carbonate Rocks of
    Northeastern British Columbia", Can. Jour. Earth Sci.,
    v. 15, pp. 1391-1406

Murray, M., and Condie, K.C., 1973, "Post Ordovician to
    Early Mesozoic History of the Eastern Klamath
    Subprovince, Northern California", Jour. Sed. Pet., v.
    43, pp. 505-515

Neelakantam, S., and Sabyasachi, R., 1979, "Barytes
    Deposits of Cuddepah Basin:, Rec. Geol. Surv. India,
    v. 112, pp. 51-63

Palache, C., Berman, H., and Frondel, C., 1951, System of
    Mineralogy, 7th ed., 2, John Wiley

Poole, F.G., Sandberg, C.A., and Boucot, A.J., 1977,
    "Silurian and Devonian Paleogeography of the Western
    United States", in: Stewart, J.H., Stevens, C.H., and
    Fritsche, A.E., eds., Paleozoic Paleogeography of the
    Western United States, SEPM, Pacific Section, Pacific
    Coast Paleogeography Symposium 1, pp. 39-66

_____, Ketner, K.B., and Smith, J.F., 1981, "Bedded Barite in Mississippian Rocks of Northeastern Nevada", U.S.G.S. Research 1981, U.S.G.S. Prof. paper 1275, p. 74

Puchelt, H., 1972, "Barium", in: Wedepohl, K.H., ed., Handbook of Geochemistry, v. 2, Springer

Potter, A.W., Hotz, P.E., and Rohr, D.M., 1977, "Stratigraphic and inferred Tectonic Framework of Lower Paleozoic Rocks in the Eastern Klamath Mountains, Northern California", in: Stewart, J.H., Stevens, C.H., and Fritsche, A.E., eds., Paleozoic Paleogeograhy of the Western United States, SEPM, Pacific Section, Pacific Coast Paleogeography Symposium 1, pp. 421-440

Rosler, N.J., and Lange, H., 1972, Geochemical Tables, Elsevier

Rye, R.O., Shawe, D.R., and Poole, F.G., 1978, "Stable Isotope Studies of Bedded Barite at East Northumberland Canyon in Toquima Range, Central Nevada", U.S.G.S. Jour. of Research, v. 6, pp. 221-229

Sakai, H., and Matsubaya, O., 1974, "Isotope Geochemistry of the Thermal Waters of Japan and its bearing on the Kuroko Ore Solution", Econ. Geol., v. 69, pp. 974-981

Savage, N.M., 1976, "Middle Devonian Species of Polygnathus from the Kennett Formation, Northern California", Jour. Paleont., v. 50, pp. 374-380

Schweickert, R.A., 1981, "Tectonic Evolution of the Sierra Nevada Range", in Ernst, W.G., ed., The Geotectonic Development of California, Rubey v. 1, pp. 87-131, Prentice Hall

_____, and Snyder, W.S., 1981, "Paleozoic Plate Tectonics of the Sierra Nevada and Adjacent Regions", in: Ernst, W.G., ed., The Geotectonic Development of California, Rubey v. 1, pp. 182-202, Prentice-Hall

Shawe, D.R., Poole, F.G., and Brobst, D.A., 1969, "Newly Discovered Bedded Barite Deposits in East Northumberland Canyon, Nye County, Nevada", Econ. Geol., v. 64, pp. 245-254

Smith, J.P., 1894, "Metamorphic Series of Shasta County", Jour. of Geol., v. 2, pp. 588-612

Snyder, W.S., 1978, "Manganese Deposited by Submarine Hot Springs in Chert-Greenstone Complexes, Western United States", Geology, v. 6, pp. 741-744

Speed, R.C., 1979, "Collided Paleozoic Microplate in the Western United States", Jour. of Geol., v. 87, pp. 279-292

Standlee, L.A., 1977, "Structure and Stratigraphy of the Shoo Fly Formation, Northern Sierra Nevada", G.S.A. Abstracts w/Progs. v. 9, p. 507

Stanley, R.C., 1961, "Counting Statistics in X-ray Spectroscopy", Brit. Jour. App. Phys., v. 12, pp. 503-506

Tafuri, B., 1973, "A Geochemical Study of the Barite Deposits of Mineral County, Nevada", M.S. thesis, Univ. of Nevada, Reno

Tieman, D.J., and Kopp, O.C., 1983, "Deformation Fabrics in Barite and Fluorite of the Del Rio District: Their Implications for the Relative Timing of Mineralization and Deformation", Econ. Geol., v. 78, pp. 91-104

Tischendorf, G., 1963, "Uber $SrSO_4$-gehalte im Baryt als ein Kriterium fur dessen bildungs bedingungen", Symposium: Problems of Postmagmatic Ore Deposition, v. 1, Prague

Turner, H.W., 1894, "The Rocks of the Sierra Nevada", U.S.G.S. 14th Annual Rept. Part II, pp. 441-495

_____, 1896, "Further Contributions to the Geology of the Sierra Nevada", U.S.G.S. 17th Annual Rept. Part I, pp. 529-656

_____, 1897, Geologic Atlas of the United States: Downieville Folio, California, U.S.G.S. Geologic Atlas Folio no. 37

Turner, J.S., and Gustafson, L.B., 1978, "The Flow of Hot Saline Solutions from Vents in the Sea Floor - some Implications for Exhalative Sulfide Deposits", Econ. Geol., v. 73, pp. 1082-1100

Urabe, T., and Sato, T., 1978, "Kuroko Deposits of the Kosaka Mine, Northeast Honshu, Japan - Products of Submarine Hot Springs on the Miocene Sea Floor", Econ. Geol., v. 73, pp. 161-178

Varga, R.J., 1980, "Structural and Tectonic Evolution of the Early Paleozoic Shoo Fly Formation, Northern Sierra Nevada Range, California", Ph.D. thesis, U.C. Davis

_____, and Moores, E.M., 1981, "Age, Origin, and Significance of an Unconformity that Predates Island Arc Volcanism in the Northern Sierra Nevada", Geology, v. 9, pp. 512-518

Volbroth, A., 1963, "Total Instrumental Analysis of Rocks", Nev. Bureau of Mines Rept. no. 6, 72 p.

Walton, A.G., 1967, The Formation and Properties of Precipitates, Interscience

Watkins, R.L., and Stensrud, H.L., 1983, "Age of Sulfide Ores in the West Shasta and East Shasta Districts, Klamath Mountains, California", Econ. Geol., v. 78, pp. 340-343

Weber, H.F., 1963, "Barite in California", Calif. Div. Mines and Geol., Miner. Info. Serv. v. 16, pp. 1-10

_____, and Matthews, R.A., 1967, "Prospecting for Barite in Northern Shasta County", Calif. Div. Mines and Geol., Miner. Info. Serv., v. 20, pp. 107-114

Wells, F.G., Walker, G.W., and Merriam, C.W., 1959, "Upper Ordovician (?) and Upper Silurian Formations of the Northern Klamath Mountains, California", G.S.A. Bull., v. 70, pp. 645-649

Zimmerman, R.A., 1965, "The Origin of the Bedded Arkansas Barite Deposits (with Special Reference to the Genetic Value of Sedimentary Features in the Ore)", Ph.D. thesis, Univ. of Missouri

_____, 1976, "Rhythmicity of Barite-Shale and of Sr in Stratabound Deposits of Arkansas", in: Wolf, K.H., ed., Handbook of Stratabound and Stratform Ore Deposits, 3, pp. 339-353, Elsevier.